

A DERIVATIVE-FREE SADDLE-SEARCH ALGORITHM WITH LINEAR CONVERGENCE RATE*

QIANG DU[†], BAOMING SHI[‡], LEI ZHANG[§], AND XIANGCHENG ZHENG[¶]

Abstract. We propose a derivative-free saddle-search algorithm designed to locate transition states using only function evaluations. The algorithm employs a nested architecture consisting of an inner eigenvector search and an outer saddle-point search. Through rigorous numerical analysis, we prove the almost sure convergence of the inner step under suitable assumptions. Furthermore, we establish the convergence of the outer search using a decaying step size, while demonstrating linear convergence under constant step size and boundedness conditions. Numerical experiments are provided to validate our theoretical results and demonstrate the algorithm's practical applicability.

Key words. saddle point, derivative-free algorithms, almost sure convergence

AMS subject classifications. 65C20, 65K10, 65L20, 37N30

1. Introduction. A recurring theme across many problems in the natural sciences and engineering is that the energy (free energy or objective functions) defined over a system's physical variables exhibits a complex landscape characterized by numerous local minima and saddle points. Examples include the phase transformations [18, 28], chemical reactions [11], protein folding [37, 46], and the loss landscapes of deep neural networks [17, 26]. While the local minima correspond to stable states, the saddle points represent transition or excited states, playing a crucial role in determining transition pathways between minima [52] and revealing the hierarchical structure of the energy landscape [47]. These features have attracted significant attention to the computation of saddle points over the past decades.

Compared with the identification of stable minima, the computation of saddle points is considerably more challenging, due to the apparent loss of stability. Moreover, the unstable directions of saddle points are in general not known beforehand. Extensive numerical algorithms have been developed to compute saddle points, which can be generally divided into two classes: path-finding methods [9, 10] and surface-walking methods [52]. We focus on the latter type, which often employs first- or second-order derivatives to evolve an iteration on the energy surface toward saddle points. Examples of this type of method include the gentlest ascent dynamics [12, 38, 30] and the high-index saddle dynamics [48, 44], which require evaluating gradients (and Hessians) of the objective function. The dimer method and the shrinking dimer dynamics [20, 50, 51] adopted a two-point gradient difference to approximate the projected Hessian in a one-dimensional space (determined by the *dimer* direction).

*The work was partially supported by NSF DMS-2309245 (for QD and BS); the National Key Research and Development Program of China 2024YFA0919500, and National Natural Science Foundation of China No. 12225102, T2321001, 12288101, and 12426653 (for LZ); the Natural Science Foundation of Shandong Province (ZR2025QB01), the National Natural Science Foundation of China (12301555), the National Key R&D Program of China (2023YFA1008903), and the Taishan Scholars Program of Shandong Province (tsqn202306083) (for XZ). Author names are sorted alphabetically.

[†]Department of Applied Physics and Applied Mathematics, and Data Science Institute, Columbia University, New York, NY 10027, USA (qd2125@columbia.edu).

[‡]Corresponding author. Department of Applied Physics and Applied Mathematics, Columbia University, New York, NY 10027, USA (bs3705@columbia.edu).

[§]Beijing International Center for Mathematical Research, Center for Quantitative Biology, Center for Machine Learning Research, Peking University, Beijing 100871, China (zhangl@math.pku.edu.cn).

[¶]School of Mathematics, State Key Laboratory of Cryptography and Digital Economy Security, Shandong University, Jinan, 250100, China (xzheng@sdu.edu.cn).

While this avoids the explicit use of the Hessian, the gradient of the energy is still needed. Thus, due to the dependence on the derivative information, these methods are not directly applicable to problems where such information might be unavailable or are difficult to access, e.g., distributed learning [27], the free energy surface in molecular simulations [33], which is not an explicit function of atomic coordinates but rather a statistical average over microscopic states, hyperparameter tuning in machine learning [43], and empirical objective function from science problems [8, 19]. We refer to [2, 39] for other practical problems where first- and higher-order derivatives are unavailable or difficult to access. Therefore, the development of derivative-free algorithms for computing saddle points is of great importance.

Zeroth-order algorithms, which rely solely on function evaluations, are applicable to the aforementioned problems and are also referred to as derivative-free or black-box methods. For example, the (stochastic) zeroth-order algorithm has been widely developed and used in optimization problems [6, 25]. However, very few works have extended zeroth-order methods to the saddle-point computation. Compared with zeroth-order optimization algorithms, zeroth-order saddle-search algorithms involve additional challenges for both algorithm design and convergence analysis. From the perspective of algorithm design, a zeroth-order saddle-search algorithm should also account for the update of unstable directions (i.e., eigenvectors of the Hessian corresponding to the negative eigenvalues) that are unknowns associated with the iterates in the configuration space. This means the second-order information needs to be reconstructed from the zeroth-order information, which may lead to the curse of dimensionality [21, 35]. From the perspective of convergence analysis, we need to deal with the iteration of both the configuration and the unstable subspace in the saddle-search algorithms, and the objective function containing saddle points is necessarily nonconvex, which may pose challenges for proving convergence. The main contribution of this paper is to derive a zeroth-order saddle-search algorithm with convergence analysis, which is applicable to many practical problems. Notably, both our theoretical and numerical results show that the iteration points of the proposed zeroth-order algorithm with constant step size approach the saddle point with a linear convergence rate, which is comparable to that of traditional (discretized) saddle dynamics, while requiring only function evaluations.

The paper is organized as follows. In [Section 2](#), we review the concept of saddle points and the saddle dynamics. In [Section 3](#), we first present the zeroth-order eigenvector-search algorithm, followed by the zeroth-order saddle-search algorithm. We establish their convergence analysis in [Section 4](#). [Section 5](#) presents numerical experiments on several benchmarks and practical problems to substantiate the theoretical results. We finally present our conclusion and discussion in [Section 6](#).

2. Saddle point and saddle dynamics. Consider a system characterized by a smooth energy function $f(\mathbf{x}) : \mathbb{R}^d \rightarrow \mathbb{R}$ with $d \geq 2$, which we assume that f is C^6 continuous. A critical point \mathbf{x}^* is defined as a configuration where the gradient vanishes, i.e., $\nabla f(\mathbf{x}^*) = 0$. The local stability of \mathbf{x}^* can be identified from the Hessian matrix $\nabla^2 f(\mathbf{x}^*)$. If $\nabla^2 f(\mathbf{x}^*)$ is positive definite, then \mathbf{x}^* is a local minimum [36]; If $\nabla^2 f(\mathbf{x}^*)$ has $k \leq d - 1$ negative eigenvalues with the corresponding k eigenvectors, denoted by $\{\mathbf{v}_1^*, \dots, \mathbf{v}_k^*\}$, \mathbf{x}^* is classified as an index- k saddle point, and $\{\mathbf{v}_1^*, \dots, \mathbf{v}_k^*\}$ referred to as “unstable eigenvectors” or “unstable directions” in this paper.

Here, we consider a particular version of the saddle dynamics for searching an

index- k saddle point \mathbf{x}^* , defined as

$$(2.1) \quad \dot{\mathbf{x}} = - \left(\mathbf{I} - 2 \sum_{i=1}^k \mathbf{v}_i \mathbf{v}_i^\top \right) \nabla f(\mathbf{x}),$$

where $\{\mathbf{v}_i\}_{i=1}^k, 1 \leq i \leq d-1$ is the normalized eigen-basis corresponding to the k smallest eigenvalues of $\nabla^2 f(\mathbf{x})$, and \mathbf{I} is the identity operator. Unlike gradient flow, which evolves along the negative gradient and causes the objective function to decrease, the right-hand side of the saddle-point dynamics applies Householder transformations to the negative gradient along the unstable directions. As a result, energy increases along the unstable directions while decreasing along the stable directions, enabling the dynamics to locate saddle points. The eigen-basis $\{\mathbf{v}_i\}_{i=1}^k$ in (2.1) can be given by an eigen-solver of $\nabla^2 f(\mathbf{x})$ which generates the unstable directions.

Using the simplest time discretization of the saddle dynamics (2.1), we get the following discrete dynamics: given $\mathbf{x}(0)$,

$$(2.2) \quad \mathbf{x}(n+1) = \mathbf{x}(n) - \alpha(n) \left(\mathbf{I} - 2 \sum_{i=1}^k \mathbf{v}_i(n) \mathbf{v}_i(n)^\top \right) \nabla f(\mathbf{x}(n)), \quad n \geq 0,$$

where $\{\mathbf{v}_i(n)\}_{i=1}^k = \text{EigenSolver}(\nabla^2 f(\mathbf{x}(n)))$, and $\alpha(n)$ is the step size.

3. Derivative-free/Zeroth-order saddle search. The iteration (2.2) requires the evaluation of the gradient and Hessian of the objective function at each step, which might be infeasible in practice or computationally expensive [2, 39]. We consider a derivative-free saddle-search algorithm that requires only zeroth-order function evaluations by employing stochastic difference approximations.

3.1. Zeroth-order approximations of the derivatives. A natural approach to derive a zeroth-order saddle-search algorithm is to substitute $\nabla f(\mathbf{x})$ and $\nabla^2 f(\mathbf{x})$ in (2.2) with zeroth-order estimators $F(\mathbf{x}, \mathbf{r}, l)$ and $\mathbf{H}(\mathbf{x}, \mathbf{r}, l)$. Here, we use a derivative-free formulation based on a two-point random zeroth-order gradient estimator, which has been widely used in the zeroth-order (derivative-free) optimization methods [35, 29, 3]. It is defined by

$$(3.1) \quad F(\mathbf{x}, \mathbf{r}, l) = \frac{f(\mathbf{x} + l\mathbf{r}) - f(\mathbf{x} - l\mathbf{r})}{2l} \mathbf{r}, \quad \mathbf{r} \sim \mathcal{N}(\mathbf{0}, \mathbf{I}),$$

where $1 \gg l > 0$ is a difference length, similar to the dimer length [20, 50], \mathbf{r} are i.i.d. random directions drawn from the standard normal distribution or a uniform distribution over a unit sphere (in this case, we need to multiply F by d [40, 16]). For $l > 0$, although the zeroth-order gradient estimator introduces bias to the true gradient, it remains unbiased to the gradient of a so-called Gaussian smoothing function with parameter l , which is defined by

$$(3.2) \quad f_l(\mathbf{x}) = \mathbb{E}_{\mathbf{r} \sim \mathcal{N}(\mathbf{0}, \mathbf{I})} (f(\mathbf{x} + l\mathbf{r})).$$

From Stein's Lemma, $\nabla f_l(\mathbf{x}) = \mathbb{E}_{\mathbf{r} \sim \mathcal{N}(\mathbf{0}, \mathbf{I})} [\nabla f(\mathbf{x} + l\mathbf{r})] = \frac{1}{l} \mathbb{E}_{\mathbf{r} \sim \mathcal{N}(\mathbf{0}, \mathbf{I})} [f(\mathbf{x} + l\mathbf{r})\mathbf{r}]$, and (3.1) is actually a two-point sampling, thus, it is unbiased gradient estimator of $f_l(\mathbf{x})$. We note that for the saddle-point search, dimer methods [20, 50, 51] adopted gradient differences to approximate the projected Hessian in the dimer direction. However, the dimer directions are not randomly sampled, and the methods are still gradient-based. We can also use (3.2) to get a derivative-free approximation of the Hessian,

$\nabla^2 f_l(\mathbf{x}) = \frac{1}{l^2} \mathbb{E}_{\mathbf{r} \sim \mathcal{N}(\mathbf{0}, \mathbf{I})}[(\mathbf{r}\mathbf{r}^\top - \mathbf{I})f(\mathbf{x} + l\mathbf{r})] = \frac{1}{l^2} \mathbb{E}_{\mathbf{r} \sim \mathcal{N}(\mathbf{0}, \mathbf{I})}[(\mathbf{r}\mathbf{r}^\top - \mathbf{I})(f(\mathbf{x} + l\mathbf{r}) - f(\mathbf{x}))].$ Consequently, the discrete sampling

$$(3.3) \quad \mathbf{H}(\mathbf{x}, \mathbf{r}, l) = \frac{f(\mathbf{x} + l\mathbf{r}) + f(\mathbf{x} - l\mathbf{r}) - 2f(\mathbf{x})}{2l^2} (\mathbf{r}\mathbf{r}^\top - \mathbf{I}), \quad \mathbf{r} \sim \mathcal{N}(\mathbf{0}, \mathbf{I}),$$

is the unbiased zeroth-order Hessian estimator of $f_l(\mathbf{x})$.

3.2. A zeroth-order/derivative-free saddle search algorithm. From (2.2), the saddle-search algorithm consists of two components:

- The inner iteration, which is the eigenvector-search algorithm that identifies the unstable directions at each iteration point, see [Algorithm 3.1](#); and
- The outer iteration, which is the saddle-search algorithm that updates the iterate by reflecting the zeroth-order gradient estimator along the unstable directions obtained from the inner step, see [Algorithm 3.2](#).

We first consider the derivative-free version of the gradient descent applied to the Rayleigh quotient for the eigenvector-search, with $\nabla^2 f(\mathbf{x})$ replaced by the zeroth-order Hessian estimator \mathbf{H} defined in (3.3): for $n \geq 0$ and $\bar{k} = 2, \dots, k$,

$$(3.4) \quad \begin{aligned} \hat{\mathbf{v}}(n+1) &= \mathbf{v}(n) - \alpha(n)(\mathbf{I} - \mathbf{v}(n)\mathbf{v}(n)^\top)\mathbf{H}(\mathbf{x}, \mathbf{r}(n), l(n))\mathbf{v}(n), \\ \mathbf{v}(n+1) &= \hat{\mathbf{v}}(n+1)/\|\hat{\mathbf{v}}(n+1)\|_2, \end{aligned}$$

$$(3.5) \quad \begin{aligned} \hat{\mathbf{v}}_{\bar{k}}(n+1) &= \mathbf{v}_{\bar{k}}(n) - \alpha(n)(\mathbf{I} - V_{n, \bar{k}} V_{n, \bar{k}}^\top)\mathbf{H}(\mathbf{x}, \mathbf{r}(n), l(n))\mathbf{v}_{\bar{k}}(n), \\ \mathbf{v}_{\bar{k}}(n+1) &= \hat{\mathbf{v}}_{\bar{k}}(n+1)/\|\hat{\mathbf{v}}_{\bar{k}}(n+1)\|_2, \end{aligned}$$

where $V_{n, \bar{k}} = [\mathbf{v}(n), \mathbf{v}_1, \dots, \mathbf{v}_{\bar{k}-1}]$, and the step size $\alpha(n) > 0$ satisfies, unless otherwise noted, the following conventional assumption.

ASSUMPTION 3.1 (Diminishing step size). $\sum_{n=0}^{\infty} \alpha(n) = \infty$, and $\sum_{n=0}^{\infty} \alpha(n)^2 < \infty$.

However, in [Subsection 4.2](#), we will show that the variation of $\mathbf{H}(\mathbf{x}, \mathbf{r}, l)$ suffers from the curse of dimensionality, which in turn slows down convergence. In (3.4) and (3.5), it suffices to adopt an approximated Hessian-vector product [50]. That is,

$$(3.6) \quad H_{\mathbf{v}}(\mathbf{x}, \mathbf{r}, l) = \frac{F(\mathbf{x} + l\mathbf{v}, \mathbf{r}, l) - F(\mathbf{x} - l\mathbf{v}, \mathbf{r}, l)}{2l}$$

can be used to replace $\mathbf{H}(\mathbf{x}, \mathbf{r}, l)\mathbf{v}$, resulting in a lower variation. Because $F(\mathbf{x}, \mathbf{r}, l)$, $\mathbf{H}(\mathbf{x}, \mathbf{r}, l)\mathbf{v}$, and $\mathbf{H}_{\mathbf{v}}(\mathbf{x}, \mathbf{r}, l)$ are biased estimators of $\nabla f(\mathbf{x})$ or $\nabla^2 f(\mathbf{x})\mathbf{v}$, we sometimes need the following diminishing difference length $l(n)$ to control the biased errors.

ASSUMPTION 3.2. *There exists a constant $L > 0$ such that $l(n) \leq L\sqrt{\alpha(n)}$.*

Based on the discrete dynamics (3.4) and (3.5) and the zeroth-order Hessian-vector product estimator $H_{\mathbf{v}}(\mathbf{x}, \mathbf{r}, l)$, we propose the zeroth-order eigenvector-search algorithm in [Algorithm 3.1](#). With the [Algorithm 3.1](#), we present [Algorithm 3.2](#) to implement the outer iteration for the derivative-free saddle-search, followed by its convergence analysis. Before we proceed to discuss the convergence of the algorithm, we present some assumptions and technical results in the rest of the section.

3.3. Assumptions on the energy. For brevity, we consider an objective function $f(\mathbf{x})$ that satisfies the following regularity assumptions.

Algorithm 3.1 Derivative-free eigenvector-search algorithm for k unstable directions

```

Initial condition:  $n \leftarrow 0$ ,  $\mathbf{v}_i, i = 1, \dots, k$ 
for  $n \leq n_{\mathbf{v}}^{max}$  do
   $\mathbf{r}$  is drawn from  $\mathcal{N}(\mathbf{0}, \mathbf{I})$ 
   $\mathbf{v}_1 \leftarrow \mathbf{v}_1 - \alpha_{\mathbf{v}}(n)(\mathbf{I} - \mathbf{v}_1 \mathbf{v}_1^\top)H_{\mathbf{v}_1}(\mathbf{x}, \mathbf{r}, l(n))$ 
   $\mathbf{v}_1 \leftarrow \mathbf{v}_1 / \|\mathbf{v}_1\|_2$ ,  $n \leftarrow n + 1$ 
end for
for  $j$  in  $\{2, \dots, k\}$  do
   $n \leftarrow 0$ 
   $\mathbf{v}_j \leftarrow \mathbf{v}_j - (\mathbf{I} - \sum_{i=1}^{j-1} \mathbf{v}_i \mathbf{v}_i^\top) \mathbf{v}_j$ ,  $\mathbf{v}_j \leftarrow \mathbf{v}_j / \|\mathbf{v}_j\|_2$ 
  for  $n \leq n_{\mathbf{v}}^{max}$  do
     $\mathbf{r}$  is drawn from  $\mathcal{N}(\mathbf{0}, \mathbf{I})$ 
     $\mathbf{v}_j \leftarrow \mathbf{v}_j - \alpha_{\mathbf{v}}(n)(\mathbf{I} - \mathbf{v}_j \mathbf{v}_j^\top - \sum_{i=1}^{j-1} \mathbf{v}_i \mathbf{v}_i^\top)H_{\mathbf{v}_j}(\mathbf{x}, \mathbf{r}, l(n))$ 
     $\mathbf{v}_j \leftarrow \mathbf{v}_j / \|\mathbf{v}_j\|_2$ ,  $n \leftarrow n + 1$ 
  end for
end for
end for

```

Algorithm 3.2 Derivative-free saddle-search algorithm for index- k saddle points

```

Initial condition:  $n \leftarrow 0$ ,  $\mathbf{x}, \mathbf{v}_i, i = 1, \dots, k$ 
for  $n \leq n_{\mathbf{x}}^{max}$  do
   $\mathbf{r}$  is drawn in  $\mathcal{N}(\mathbf{0}, \mathbf{I})$ 
   $\mathbf{x} \leftarrow \mathbf{x} - \alpha_{\mathbf{x}}(n)(\mathbf{I} - \sum_{i=1}^k 2\mathbf{v}_i \mathbf{v}_i^T)F(\mathbf{x}, \mathbf{r}, l(n))$ 
  Searching  $k$  unstable directions  $\{\mathbf{v}_i\}_{i=1}^k$  of  $\nabla^2 f(\mathbf{x})$  with Algorithm 3.1
   $n \leftarrow n + 1$ 
end for

```

ASSUMPTION 3.3. Assume $f \in C^6$, for all $\mathbf{x} \in \mathbb{R}^n$, we have $\|\nabla^i f(\mathbf{x})\|_2 \leq M$ for a positive constant $M < \infty$, and $i = 2, 3, 4, 5, 6$.

Remark 3.1. For the analysis of the saddle-search algorithm, taking the simplest quadratic function as an example, we can impose uniform boundedness of higher-order derivatives as in [54, 53]. In many applications, there exist various objective functions satisfying Assumption 3.3, such as the Minyaev-Quapp energy function [34] and the Eckhardt energy function [13].

ASSUMPTION 3.4. There exist $\delta > 0$ and $\mu \in (0, M)$, such that $\forall \mathbf{x} \in \{\mathbf{x}, \|\mathbf{x} - \mathbf{x}^*\|_2 \leq \delta\}$, the eigenvalues of $\nabla^2 f(\mathbf{x})$ satisfy

$$(3.7) \quad -M \leq \lambda_1 \leq \dots \leq \lambda_k < -\mu < 0 < \mu < \lambda_{k+1} \leq \dots \leq \lambda_d \leq M.$$

Remark 3.2. The eigenvalue assumption holds for every strict saddle point \mathbf{x}^* . From Assumption 3.3, the L_2 -norm of the Hessian is uniformly bounded by M . Moreover, from Assumption 3.3, for any \mathbf{v} that satisfies $\|\mathbf{v}\|_2 = 1$, we have

$$\|(\nabla^2 f(\mathbf{x}) - \nabla^2 f(\mathbf{y}))\mathbf{v}\|_2 = \left\| \int_0^1 \nabla^3 f(\mathbf{y} + t(\mathbf{x} - \mathbf{y}))[\mathbf{x} - \mathbf{y}, \mathbf{v}] dt \right\|_2 \leq M \|\mathbf{x} - \mathbf{y}\|_2,$$

which gives the Lipschitz condition $\|\nabla^2 f(\mathbf{x}) - \nabla^2 f(\mathbf{y})\|_2 \leq M \|\mathbf{x} - \mathbf{y}\|_2$, $\forall \mathbf{x}, \mathbf{y} \in U$, with the constant M being specified in Assumption 3.3.

3.4. Estimates on the approximate gradient and Hessian. The following lemma demonstrates that the second-order moments of the zeroth-order gradient and Hessian are bounded in any bounded domain $\{\mathbf{x}, \|\mathbf{x}\|_2 \leq C\}$.

LEMMA 3.3 (Almost unbiased estimator). *Under Assumption 3.3, we have*

$$\begin{aligned} \mathbb{E}_{\mathbf{r}}[F(\mathbf{x}, \mathbf{r}, l)] &= \nabla f_l(\mathbf{x}), \mathbb{E}_{\mathbf{r}}[\mathbf{H}(\mathbf{x}, \mathbf{r}, l)] = \nabla^2 f_l(\mathbf{x}), \\ \mathbb{E}_{\mathbf{r}}[\|F(\mathbf{x}, \mathbf{r}, l)\|_2^2] &\leq (2d+4)\|\nabla f(\mathbf{x})\|_2^2 + \frac{M^2 l^4 d(d+2)(d+4)(d+6)}{18}, \\ \mathbb{E}_{\mathbf{r}}[\|\mathbf{H}(\mathbf{x}, \mathbf{r}, l)\|_2^2] &\leq \frac{M^2 d(d+2)(d^2+12d+33)}{2} \\ &\quad + \frac{M^2 l^4 d(d+2)(d+4)(d+6)(d^2+20d+97)}{288}, \\ (3.8) \quad \|\nabla f(\mathbf{x}) - \nabla f_l(\mathbf{x})\|_2 &\leq \frac{Ml^2 d}{2}, \|\nabla^2 f(\mathbf{x}) - \nabla^2 f_l(\mathbf{x})\|_2 \leq \frac{Ml^2 d}{2}. \end{aligned}$$

Proof. This Lemma follows directly from the Taylor expansion and the higher-order moments of the normal distribution, with the proof provided in the Appendix. \square

LEMMA 3.4. *Under Assumption 3.3 and Assumption 3.4, $\nabla^2 f_l(\mathbf{x})$ is Lipschitz continuous. Moreover, if $Ml^2 d/2 \ll 1$, its eigenvalue satisfies that, for $\mu_l = \mu - Ml^2 d/2 > 0$ and any $\mathbf{x} \in \{\mathbf{x}, \|\mathbf{x} - \mathbf{x}^*\|_2 \leq \delta\}$,*

$$(3.9) \quad -M \leq \lambda_1 \leq \cdots \leq \lambda_k < -\mu_l < 0 < \mu_l < \lambda_{k+1} \leq \cdots \leq \lambda_d \leq M.$$

Proof. To verify the Lipschitz continuity of $\nabla^2 f_l(\mathbf{x})$, we compute

$$\|\nabla^2 f_l(\mathbf{x}) - \nabla^2 f_l(\mathbf{y})\|_2 = \|\mathbb{E}_{\mathbf{r}}[\nabla^2 f(\mathbf{x} + l\mathbf{r}) - \nabla^2 f(\mathbf{y} + l\mathbf{r})]\|_2 \leq M\|\mathbf{x} - \mathbf{y}\|_2.$$

From Assumption 3.3, we have that

$$\|\nabla^i f_l(\mathbf{x})\|_2 = \|\mathbb{E}_{\mathbf{r}}[\nabla^i f(\mathbf{x} + l\mathbf{r})]\|_2 \leq \mathbb{E}_{\mathbf{r}}[\|\nabla^i f(\mathbf{x} + l\mathbf{r})\|_2] \leq M, i = 2, 3, 4, 5, 6.$$

Then, (3.9) is a direct sequence of (3.8), Assumption 3.3, and Assumption 3.4. \square

We generally require the difference length l to be sufficiently small, which is specified by the following assumption.

ASSUMPTION 3.5. *The difference length l satisfies $dl \ll 1, Ml^2 d/2 \ll 1$.*

3.5. Some technical results. We first quote a classical result on the perturbation of the matrix eigenvalue problem, which will be used to assess the approximation of the unstable subspace of the Hessian.

LEMMA 3.5 (Davis-Kahan theorem [49]). *Let $\Sigma, \hat{\Sigma} \in \mathbb{R}^{d \times d}$ be symmetric matrices, with eigenvalues $\lambda_d \geq \cdots \geq \lambda_1$ and $\hat{\lambda}_d \geq \cdots \geq \hat{\lambda}_1$ respectively. Fix $1 \leq r \leq s \leq d$ and assume that $\min(\lambda_r - \lambda_{r-1}, \lambda_{s+1} - \lambda_s) > 0$, where we define $\lambda_0 = -\infty$ and $\lambda_{d+1} = +\infty$. Let $p = s - r + 1$, and let $V = [\mathbf{v}_r, \mathbf{v}_{r+1}, \dots, \mathbf{v}_s] \in \mathbb{R}^{d \times p}$ and $\hat{V} = [\hat{\mathbf{v}}_r, \hat{\mathbf{v}}_{r+1}, \dots, \hat{\mathbf{v}}_s] \in \mathbb{R}^{d \times p}$ have orthonormal columns satisfying $\Sigma \mathbf{v}_j = \lambda_j \mathbf{v}_j$, $\hat{\Sigma} \hat{\mathbf{v}}_j = \hat{\lambda}_j \hat{\mathbf{v}}_j$, and $\|\mathbf{v}_j\|_2 = \|\hat{\mathbf{v}}_j\|_2 = 1$, for $j = r, r+1, \dots, s$. Then*

$$\|VV^\top - \hat{V}\hat{V}^\top\|_F \leq \frac{2\sqrt{2} \min(p^{1/2} \|\hat{\Sigma} - \Sigma\|_2, \|\hat{\Sigma} - \Sigma\|_F)}{\min(\lambda_r - \lambda_{r-1}, \lambda_{s+1} - \lambda_s)}.$$

To help us prove the convergence of the saddle-search algorithm, we quote [42, Lemma 4.3] on the convergence of a noisy recursive process.

LEMMA 3.6. *Let $A(\mathbf{x}) : \mathbb{R}^d \rightarrow \mathbb{R}$ be a function bounded from below, $B(\mathbf{x}) : \mathbb{R}^d \rightarrow \mathbb{R}$ be a non-negative function, i.e., $B(\mathbf{x}) \geq 0$ for all $\mathbf{x} \in \mathbb{R}^d$, $\mathcal{F}(n)$ denote the filtration generated by the random variables $\mathcal{F}(n) = \{\mathbf{x}_0, \mathbf{x}_1, \dots, \mathbf{x}_n\}$. With step size assumption in Assumption 3.1, suppose there exist constants $C_1, C_2 > 0$ such that*

$$(3.10) \quad \mathbb{E}(A(\mathbf{x}(n+1)) - A(\mathbf{x}(n))|\mathcal{F}(n)) \leq -C_1\alpha(n)B(\mathbf{x}(n)) + C_2\alpha(n)^2,$$

then $A(\mathbf{x}(n))$ almost surely converges as $n \rightarrow \infty$. If $B(\mathbf{x}(n))$ also converges almost surely, then it almost surely converges to zero.

4. Convergence of the derivative-free saddle search algorithm. We first study in Subsection 4.1 the convergence of the eigenvector-search algorithm with the Hessian estimator. We also study the effect of dimensionality on the convergence in Subsection 4.2, and study the convergence of the inner eigenvector-search algorithm Algorithm 3.1 in Subsection 4.3. Then, based on the unstable directions output by the inner iteration, we analyze in Subsection 4.4 the convergence of the outer iteration, that is, the derivative-free saddle-search algorithm (Algorithm 3.2).

4.1. Convergence of the inner derivative-free eigenvector-search algorithm with zeroth-order Hessian estimator. For the saddle point search, the important aspect is to identify the unstable directions. Thus, the convergence of the inner iteration focuses on the convergence of the projection operator on the unstable subspaces. We note that this analysis largely follows the approach used in [42].

LEMMA 4.1. *Under Assumption 3.1 and Assumption 3.5, the limit points of $\mathbf{v}(n)$ generated by (3.4) with $l(n) \equiv l$ almost surely lie in the eigenspace of $\nabla^2 f_l(\mathbf{x})$. The limit points, $\mathbf{v}_\infty \notin \text{span}\{\mathbf{v}_{l,1}, \dots, \mathbf{v}_{l,\bar{k}-1}\}$, of the iteration points $\mathbf{v}(n)$ generated by (3.5), almost surely lie in the eigenspace of $\nabla^2 f_l(\mathbf{x})$, provided that $\mathbf{v}_{l,i}, i = 1, \dots, \bar{k}-1$ are eigenvectors of $\nabla^2 f_l(\mathbf{x})$ and $\mathbf{v}(0)$ is orthogonal to $\mathbf{v}_i, i = 1, \dots, \bar{k}-1$.*

Proof. This is a direct sequence of Lemma 3.3 and [42, Proposition 4.9]. \square

Remark 4.2. Consider the Rayleigh quotient problem

$$\min_{\mathbf{v}} \mathbf{v}^\top \nabla^2 f_l(\mathbf{x}) \mathbf{v} \text{ s.t. } \|\mathbf{v}\|^2 = 1, \mathbf{v}_{l,j}^\top \mathbf{v} = 0, j = 1, \dots, \bar{k}-1.$$

The solution to the above problem gives the eigenvector $\mathbf{v}_{l,\bar{k}}$ corresponding to the \bar{k} -th smallest eigenvalue of $\nabla^2 f_l(\mathbf{x})$, where $\mathbf{v}_{l,i}, i = 1, \dots, \bar{k}-1$ is the eigenvector corresponding to the i -th smallest eigenvalue. If $\lambda_{\bar{k}}$ is simple, $\mathbf{v}_{l,\bar{k}}$ serves as the global minimizer, and $\mathbf{v}_{l,i}, i > \bar{k}$ serve as the unstable saddle point. Even in the worst-case scenario, where the algorithm converges to a saddle point or the eigenvector corresponding to positive eigenvalues, we can repeat the eigenvector search to identify the unstable directions. Thus, in the following, we assume that the eigenspace in Lemma 4.1 is actually spanned by the k smallest eigenvectors of $\nabla^2 f_l(\mathbf{x})$.

Denote the eigenvectors corresponding to the k smallest eigenvalues of $\nabla^2 f(\mathbf{x})$ and $\nabla^2 f_l(\mathbf{x})$ by $V = [\mathbf{v}_1(\mathbf{x}), \dots, \mathbf{v}_k(\mathbf{x})]$ and $V_l = [\mathbf{v}_{1,l}(\mathbf{x}), \dots, \mathbf{v}_{k,l}(\mathbf{x})]$, respectively, and denote the outputs of (3.4) and (3.5) by $\bar{V} = [\bar{\mathbf{v}}_1, \dots, \bar{\mathbf{v}}_k]$.

LEMMA 4.3. *Suppose Assumption 3.1 holds. Given an arbitrary tolerance $\epsilon_v > 0$, \bar{V} achieves the tolerance*

$$(4.1) \quad \|\bar{V}\bar{V}^\top - V_l V_l^\top\|_2 \leq \epsilon_v,$$

in a finite number of iterations, almost surely.

Proof. This is a direct sequence of [42, Theorem 4.13]. \square

COROLLARY 4.4. *Suppose Assumption 3.1, Assumption 3.3, and Assumption 3.4 hold. If \bar{V} satisfies the tolerance in (4.1), then it is also a good approximation of V if the difference length l is small. Specifically,*

$$\|\bar{V}\bar{V}^\top - VV^\top\|_2 \leq \frac{\sqrt{2k}Ml^2d}{4\mu} + \epsilon_v.$$

Proof. By setting $\Sigma = \nabla^2 f(\mathbf{x})$, $\hat{\Sigma} = \nabla^2 f_l(\mathbf{x})$, $s = k$, $r = 1$ in Lemma 3.5, we have $\min(\lambda_{k+1} - \lambda_k, \lambda_1 - \lambda_0) \geq 2\mu$, and

$$\|V_l V_l^\top - VV^\top\|_2 \leq \|V_l V_l^\top - VV^\top\|_F \leq \frac{\sqrt{2k}}{2\mu} \|\nabla^2 f_l(\mathbf{x}) - \nabla^2 f(\mathbf{x})\|_2 \leq \frac{\sqrt{2k}Ml^2d}{4\mu},$$

$$\|\bar{V}\bar{V}^\top - VV^\top\|_2 \leq \|\bar{V}\bar{V}^\top - V_l V_l^\top\|_2 + \|V_l V_l^\top - VV^\top\|_2 \leq \frac{\sqrt{2k}Ml^2d}{4\mu} + \epsilon_v.$$

4.2. The dimensional dependence of the error. We should note that the zeroth-order Hessian estimator in (3.4) and (3.5) suffers from the curse of dimensionality. By ignoring the $O(l^4d^6)$ term which can be controlled by a small enough l in Lemma 3.3, we have

$$(4.2) \quad \mathbb{E}_\mathbf{r}[\|\mathbf{H}(\mathbf{x}, \mathbf{r}, l)\|_2^2] \lesssim \frac{d(d+2)(d^2 + 12d + 33)M^2}{2} = O(d^4).$$

In fact, $\mathbf{H}(\mathbf{x}, \mathbf{r}, l)$ contains only one-dimensional curvature information to approximate the $d \times d$ Hessian. It is therefore not surprising that the variation increases quickly as the dimension d grows. Then, we show that this large variation will slow down the convergence. Without loss of generality, we assume that $\mathbb{E}_\mathbf{r}(\|\mathbf{H}(\mathbf{x}, \mathbf{r}, l)\|_2^2) \leq C_3 d^4$. Consider the iteration in (3.4), and define Rayleigh Quotient and the squared norm of its Riemannian gradient, as $A(\mathbf{v}) = \mathbf{v}^\top \nabla^2 f(\mathbf{x}) \mathbf{v}$ and $B(\mathbf{v}) = \|(\mathbf{I} - \mathbf{v}\mathbf{v}^\top) \nabla^2 f(\mathbf{x}) \mathbf{v}\|_2^2$, then

$$\begin{aligned} & A(\mathbf{v}(n+1)) - A(\mathbf{v}(n)) \\ & \leq -2\alpha(n) \langle (\mathbf{I} - \mathbf{v}(n)\mathbf{v}(n)^\top) \mathbf{H}(\mathbf{x}, \mathbf{r}(n), l(n)) \mathbf{v}(n), (\mathbf{I} - \mathbf{v}(n)\mathbf{v}(n)^\top) \nabla^2 f_l(\mathbf{x}) \mathbf{v}(n) \rangle \\ & \quad + M_1 \alpha(n)^2 \|\mathbf{H}(\mathbf{x}, \mathbf{r}(n), l(n))\|_2^2, \end{aligned}$$

where M_1 is a positive constant dependent on M . Taking expectations on both sides,

$$\begin{aligned} & \mathbb{E}[A(\mathbf{v}(n+1)) - A(\mathbf{v}(n)) | \mathcal{F}(n)] \\ & \leq -2\alpha(n)B(\mathbf{v}(n)) + M_1 \alpha(n)^2 \mathbb{E}[\|\mathbf{H}(\mathbf{x}, \mathbf{r}(n), l(n))\|_2^2] \\ & \leq -2\alpha(n)B(\mathbf{v}(n)) + M_1 C_3 \alpha(n)^2 d^4. \end{aligned}$$

By taking expectation with respect to $\mathcal{F}(n)$, we get that

$$\mathbb{E}[A(\mathbf{v}(n+1))] - \mathbb{E}[A(\mathbf{v}(n))] \leq -2\alpha(n)\mathbb{E}[B(\mathbf{v}(n))] + M_1 C_3 \alpha(n)^2 d^4.$$

Using the telescoping argument, we obtain

$$\begin{aligned} (4.3) \quad \min_{1 \leq i \leq n} \mathbb{E}[B(\mathbf{v}(i))] & \leq \frac{A(\mathbf{v}(0)) - \mathbb{E}[A(\mathbf{v}(n+1))] + M_1 C_3 \sum_{i=0}^{\infty} \alpha(i)^2 d^4}{2 \sum_{i=0}^n \alpha(i)} \\ & \leq \frac{A(\mathbf{v}(0)) + M + M_1 C_3 \sum_{i=0}^{\infty} \alpha(i)^2 d^4}{2 \sum_{i=0}^n \alpha(i)}. \end{aligned}$$

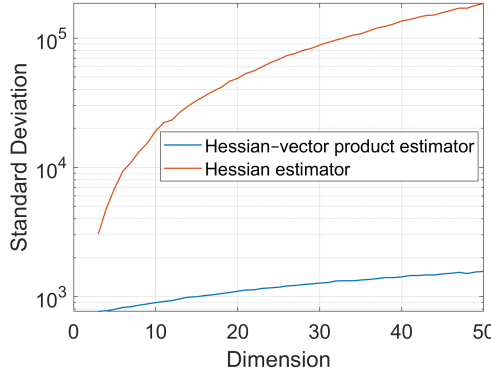


FIG. 1. The standard deviations are computed over 10000 samples of $\mathbf{H}\mathbf{v}$ (Hessian estimator) and $H_{\mathbf{v}}$ (Hessian-vector estimator), where \mathbf{v} is a fixed vector drawn from $\mathcal{N}(\mathbf{0}, \mathbf{I})$.

Hence, a larger dimension d slows down the convergence. Moreover, in Subsection 5.3, we show that the large variation also leads to potential numerical instability. Fortunately, we do not need the full Hessian information. In (3.4) and (3.5), it suffices to approximate the Hessian-vector product, $\nabla^2 f(\mathbf{x})\mathbf{v}$, which is also a key idea in [50] for avoiding any explicit Hessian evaluation. To this end, $H_{\mathbf{v}}(\mathbf{x}, \mathbf{r}, l)$ as defined by (3.6) could be used to approximate $\nabla^2 f(\mathbf{x})\mathbf{v}$.

LEMMA 4.5. *Suppose Assumption 3.3 and Assumption 3.5 hold, then*

$$\|\mathbb{E}_{\mathbf{r}}[H_{\mathbf{v}}(\mathbf{x}, \mathbf{r}, l)] - \nabla^2 f(\mathbf{x})\mathbf{v}\|_2 \leq Ml^2d,$$

$$\begin{aligned} \mathbb{E}_{\mathbf{r}}[\|H_{\mathbf{v}}(\mathbf{x}, \mathbf{r}, l)\|_2^2] &\leq 4(d+2)M^2 + \frac{M^2d(d+2)l^4}{9} \\ &\quad + \frac{M^2d(d+2)(d+4)(d+6)l^4}{9} + O(l^8d^8) \leq 10M^2d. \end{aligned}$$

Proof. The proof is given in the Appendix. \square

The use of $H_{\mathbf{v}}$ significantly reduces the variation in (4.2) from $O(d^4)$ to $O(d)$ (also see Figure 1), and accelerates the convergence of the eigenvector search.

4.3. Convergence of the inner derivative-free eigenvector-search algorithm with zeroth-order Hessian-vector estimator. The following proposition demonstrates that the output of the Algorithm 3.1 with Hessian-vector estimator $H_{\mathbf{v}}$ can serve as approximations to the unstable directions of both the original function $f(\mathbf{x})$ and the Gaussian smoothed function $f_{l_0}(\mathbf{x})$ with a small l_0 .

Denote the output of the Algorithm 3.1 by $\tilde{V} = [\tilde{\mathbf{v}}_1, \dots, \tilde{\mathbf{v}}_k]$.

PROPOSITION 4.6. *Suppose the Assumption 3.1, Assumption 3.2, and Assumption 3.3 hold. Then, for any $\epsilon_{\mathbf{v}}$, there almost surely exists a finite $n_{\mathbf{v}}^{max}$ (that depends on $\epsilon_{\mathbf{v}}$ and on the random realization of the samples $\mathbf{r}(n)$) such that the output \tilde{V} of Algorithm 3.1 satisfies $\|\tilde{V}\tilde{V}^T - VV^T\|_2 \leq \epsilon_{\mathbf{v}}$ and $\|\tilde{V}\tilde{V}^T - V_lV_l^T\|_2 \leq \epsilon_{\mathbf{v}} + \frac{\sqrt{2k}Ml_0^2d}{4\mu}$.*

Proof. The proof follows the same line as [42, Theorem 4.13], which itself relies on [42, Proposition 4.8], that is, the single-eigenvector iteration in (3.4) converges almost surely to the true unstable eigenvector. By choosing a sufficiently large n_{max} , we can ensure that the output of the algorithm is close to the true eigenvector. A key distinction here is that [42, Proposition 4.8] is proved under the assumption of

an unbiased estimator, whereas the estimate $H_{\mathbf{v}}$ is biased. We control the bias using the condition $l(n) \leq L\sqrt{\alpha(n)}$ so that the additional error introduced by the bias becomes asymptotically negligible, and the almost-sure convergence statement also carries over to our setting. To show this specifically, for any \mathbf{v} with $\|\mathbf{v}\|_2 = 1$, we define the Rayleigh Quotient as $A(\mathbf{v}) = \mathbf{v}^T \nabla^2 f(\mathbf{x}) \mathbf{v}$, then

$$\begin{aligned} & A(\mathbf{v}(n+1)) - A(\mathbf{v}(n)) \\ &= \mathbf{v}(n+1)^T \nabla^2 f(\mathbf{x}) \mathbf{v}(n+1) - \mathbf{v}(n)^T \nabla^2 f(\mathbf{x}) \mathbf{v}(n) \\ &\quad - \langle (\mathbf{I} - \mathbf{v}(n)\mathbf{v}(n)^T) H_{\mathbf{v}(n)}(\mathbf{x}, \mathbf{r}(n), l(n)), \mathbf{v}(n)\mathbf{v}(n)^T \nabla^2 f(\mathbf{x}) \mathbf{v}(n) \rangle \\ &\leq -2\alpha(n) \langle (\mathbf{I} - \mathbf{v}(n)\mathbf{v}(n)^T) H_{\mathbf{v}(n)}(\mathbf{x}, \mathbf{r}(n), l(n)), (\mathbf{I} - \mathbf{v}(n)\mathbf{v}(n)^T) \nabla^2 f(\mathbf{x}) \mathbf{v}(n) \rangle \\ &\quad + M_2 \alpha(n)^2 \|H_{\mathbf{v}(n)}(\mathbf{x}, \mathbf{r}(n), l(n))\|_2^2, \end{aligned}$$

where M_2 is a positive constant only dependent on M . Taking expectations on both sides, and utilizing [Lemma 4.5](#), we have

$$\begin{aligned} & \mathbb{E}(A(\mathbf{v}(n+1)) - A(\mathbf{v}(n)) | \mathcal{F}(n)) \\ &\leq -2\alpha(n)B(\mathbf{v}(n)) + M_2 \alpha(n)^2 \mathbb{E}_{\mathbf{r}}[\|H_{\mathbf{v}(n)}\|_2^2] \\ &\quad + 2\alpha(n) \langle (\mathbf{I} - \mathbf{v}(n)\mathbf{v}(n)^T) (\nabla^2 f(\mathbf{x}) \mathbf{v}(n) - \mathbb{E}_{\mathbf{r}}[H_{\mathbf{v}(n)}]), (\mathbf{I} - \mathbf{v}(n)\mathbf{v}(n)^T) \nabla^2 f(\mathbf{x}) \mathbf{v}(n) \rangle \\ &\leq -2\alpha(n)B(\mathbf{v}(n)) + (10dM_2M^2 + 2L^2M^2d) \alpha(n)^2, \end{aligned}$$

where $B(\mathbf{v}) = \|(\mathbf{I} - \mathbf{v}\mathbf{v}^T) \nabla^2 f(\mathbf{x}) \mathbf{v}\|_2^2$. Then, same as the proof in [\[42, Proposition 4.8\]](#), we can show that $A(\mathbf{v}(n))$ and $B(\mathbf{v}(n))$ satisfy the condition in [Lemma 3.6](#), and hence the almost sure convergence of $\mathbf{v}(n)$ to the true unstable eigenvector holds.

From [Proposition 4.6](#), we know that the iterates $\mathbf{v}(n)$ of the inner eigenvector search converges almost surely to the true unstable eigenvector. However, the number of iterations required is a random quantity that depends on the sample path. In the remainder of this subsection, we propose a more automatic stopping criterion and, for brevity, restrict to the case $k = 1$. By [\[42, Theorem 4.13\]](#), the distance between $\mathbf{v}(n)$ and the true unstable eigenvector can be controlled by the residual $\|(\mathbf{I} - \mathbf{v}(n)\mathbf{v}(n)^T) \nabla^2 f(\mathbf{x}) \mathbf{v}(n)\|_2$. This motivates us to use the zeroth-order residual $\|(\mathbf{I} - \mathbf{v}(n)\mathbf{v}(n)^T) \bar{H}_{\mathbf{v}(n)}\| < \epsilon$ as a potential stopping criterion, where

$$\bar{H}_{\mathbf{v}(n)} := \frac{1}{m} \sum_{i=1}^m H_{\mathbf{v}(n)}(\mathbf{x}, \mathbf{r}(i), l(n)).$$

In what follows, we first prove that the stopping criterion almost surely holds in a finite number of iterations. We also prove that this stopping criterion with an increasing m guarantees with a positive probability that, at each inner eigenvector search, $\|(\mathbf{I} - \mathbf{v}(n)\mathbf{v}(n)^T) \nabla^2 f(\mathbf{x}) \mathbf{v}(n)\|_2$ is sufficiently small so that the returned vector is sufficiently close to the true unstable eigenvector by [\[42, Theorem 4.13\]](#).

PROPOSITION 4.7. *Under the same conditions as in [Proposition 4.6](#), $\forall m \geq 1, \epsilon > 0$, the iteration $\mathbf{v}(n)$ satisfies the stopping criterion $\|(\mathbf{I} - \mathbf{v}(n)\mathbf{v}(n)^T) \bar{H}_{\mathbf{v}(n)}\|_2 < \epsilon$ in a finite number of iterations almost surely.*

Proof. Define the termination time $T := \inf\{n \geq 1, \|(\mathbf{I} - \mathbf{v}(n)\mathbf{v}(n)^T) \bar{H}_{\mathbf{v}(n)}\|_2 < \epsilon\}$. For each n , we decompose

$$\begin{aligned} & (\mathbf{I} - \mathbf{v}(n)\mathbf{v}(n)^T) \bar{H}_{\mathbf{v}(n)} = (\mathbf{I} - \mathbf{v}(n)\mathbf{v}(n)^T) \nabla^2 f(\mathbf{x}) \mathbf{v}(n) \\ (4.4) \quad & \quad + (\mathbf{I} - \mathbf{v}(n)\mathbf{v}(n)^T) (\mathbb{E}_{\mathbf{r}}[\bar{H}_{\mathbf{v}(n)}] - \nabla^2 f(\mathbf{x}) \mathbf{v}(n)) \\ & \quad + (\mathbf{I} - \mathbf{v}(n)\mathbf{v}(n)^T) (\bar{H}_{\mathbf{v}(n)} - \mathbb{E}_{\mathbf{r}}[\bar{H}_{\mathbf{v}(n)}]). \end{aligned}$$

By [Proposition 4.6](#), for almost every random event ω , there exists $N(\omega)$ such that, for all $n > N_1(\omega)$, $\|(\mathbf{I} - \mathbf{v}(n)\mathbf{v}(n)^\top)\nabla^2 f(\mathbf{x})\mathbf{v}(n)\|_2 < \epsilon/4$. Note that $l(n) \leq L\sqrt{\alpha(n)} \rightarrow 0$, by [Lemma 4.5](#), there exists a deterministic N_2 such that, for all $n > N_2$ (so that $l(n)$ is small enough), $\|(\mathbf{I} - \mathbf{v}(n)\mathbf{v}(n)^\top)(\mathbb{E}_\mathbf{r}[\bar{H}_{\mathbf{v}(n)}] - \nabla^2 f(\mathbf{x})\mathbf{v}(n))\|_2 < \epsilon/4$. Next, by the Taylor expansion of f at \mathbf{x} , we have for each fixed \mathbf{v} and l ,

$$H_\mathbf{v} = \frac{F(\mathbf{x} + l\mathbf{v}, \mathbf{r}, l) - F(\mathbf{x} - l\mathbf{v}, \mathbf{r}, l)}{2l} = \mathbf{r}\mathbf{r}^\top \nabla^2 f(\mathbf{x})\mathbf{v} + O(l^2),$$

where the $O(l^2)$ term is uniform in \mathbf{r} under the regularity assumptions on f . Since each $\mathbf{r}(i)$ is drawn from the standard normal distribution, when $l(n)$ is small, there exist $N_3 \in \mathbb{N}$ and a constant $\delta_p > 0$ such that, for all $n > N_3$, we have $\mathbb{P}(\|(\mathbf{I} - \mathbf{v}(n)\mathbf{v}(n)^\top)(\bar{H}_{\mathbf{v}(n)} - \mathbb{E}_\mathbf{r}[\bar{H}_{\mathbf{v}(n)}])\|_2 < \epsilon/2) \geq \delta_p$. Hence, $\forall n > N_4 = \max(N_1, N_2, N_3)$, we have $\mathbb{P}(T > n) \leq (1 - \delta_p)^{n - N_4}$, which means $\mathbb{P}(T = \infty) = 0$. \square

PROPOSITION 4.8. *Let T be the termination time, i.e., the stopping criterion $\|(\mathbf{I} - \mathbf{v}(T)\mathbf{v}(T)^\top)\bar{H}_{\mathbf{v}(T)}\| < \epsilon$ holds, and m is large enough such that $10M^2d < m\epsilon^2$, then*

$$\mathbb{P}(\|(\mathbf{I} - \mathbf{v}(T)\mathbf{v}(T)^\top)\nabla^2 f(\mathbf{x})\mathbf{v}(T)\|_2 < 2\epsilon + Ml(T)^2d) \geq 1 - \frac{10M^2d}{m\epsilon^2}.$$

Proof. From (4.4), we have that

$$\begin{aligned} & \|(\mathbf{I} - \mathbf{v}(T)\mathbf{v}(T)^\top)\nabla^2 f(\mathbf{x})\mathbf{v}(T)\|_2 \\ & \leq \|(\mathbf{I} - \mathbf{v}(T)\mathbf{v}(T)^\top)\bar{H}_{\mathbf{v}(T)}\|_2 + \|(\mathbf{I} - \mathbf{v}(T)\mathbf{v}(T)^\top)(\mathbb{E}_\mathbf{r}[\bar{H}_{\mathbf{v}(T)}] - \nabla^2 f(\mathbf{x})\mathbf{v}(T))\|_2 \\ & \quad + \|(\mathbf{I} - \mathbf{v}(T)\mathbf{v}(T)^\top)(\bar{H}_{\mathbf{v}(T)} - \mathbb{E}_\mathbf{r}[\bar{H}_{\mathbf{v}(T)}])\|_2 \\ & < \epsilon + Ml(T)^2d + \|(\mathbf{I} - \mathbf{v}(T)\mathbf{v}(T)^\top)(\bar{H}_{\mathbf{v}(T)} - \mathbb{E}_\mathbf{r}[\bar{H}_{\mathbf{v}(T)}])\|_2. \end{aligned}$$

Note that

$$\begin{aligned} & \mathbb{E}_\mathbf{r}[\|(\mathbf{I} - \mathbf{v}(T)\mathbf{v}(T)^\top)(\bar{H}_{\mathbf{v}(T)} - \mathbb{E}_\mathbf{r}[\bar{H}_{\mathbf{v}(T)}])\|_2^2] \leq \mathbb{E}_\mathbf{r}[\|\bar{H}_{\mathbf{v}(T)} - \mathbb{E}_\mathbf{r}[\bar{H}_{\mathbf{v}(T)}]\|_2^2] \\ & \leq \frac{\mathbb{E}_\mathbf{r}[\|H_{\mathbf{v}(T)} - \mathbb{E}_\mathbf{r}[H_{\mathbf{v}(T)}]\|_2^2]}{m} \leq \frac{\mathbb{E}_\mathbf{r}[\|H_{\mathbf{v}(T)}\|_2^2]}{m} \leq \frac{10M^2d}{m}, \end{aligned}$$

where the first inequality follows from the bound $\|\mathbf{I} - \mathbf{v}(T)\mathbf{v}(T)^\top\|_2 \leq 1$, the second inequality holds because $\bar{H}_{\mathbf{v}}$ is the average of m independent copies of $H_{\mathbf{v}}$, and the last inequality follows from [Lemma 4.5](#). From the Chebyshev inequality, we get

$$\mathbb{P}(\|(\mathbf{I} - \mathbf{v}(T)\mathbf{v}(T)^\top)(\bar{H}_{\mathbf{v}(T)} - \mathbb{E}_\mathbf{r}[\bar{H}_{\mathbf{v}(T)}])\|_2 \geq \epsilon) \leq \frac{10M^2d}{m\epsilon^2}.$$

COROLLARY 4.9. *Suppose the same conditions in [Proposition 4.6](#) hold. At the n -th iteration of the outer saddle algorithm, choose the sample size $m_n = O(n^p)$ with some $p > 1$ in the stopping criterion of the inner eigenvector search. That is, in the inner loop, we form $\bar{H}_{\mathbf{v}} := \frac{1}{m_n} \sum_{i=1}^{m_n} H_{\mathbf{v}}(\mathbf{x}_n, \mathbf{r}(i), l)$, $\mathbf{r}(i) \sim \mathcal{N}(\mathbf{0}, \mathbf{I})$ and stop as soon as $\|(\mathbf{I} - \mathbf{v}\mathbf{v}^\top)\bar{H}_{\mathbf{v}}\| < \epsilon$. Then, there exists a positive probability that the vector $\mathbf{v}_n(T)$ returned by the inner algorithm satisfies*

$$\|(\mathbf{I} - \mathbf{v}_n(T)\mathbf{v}_n(T)^\top)\nabla^2 f(\mathbf{x}_n)\mathbf{v}_n(T)\|_2 < 2\epsilon + Ml(0)^2d, \forall n \in \mathbb{N}.$$

Proof. Note that $l(0) \geq l(T)$ by [Assumption 3.2](#). By the [Proposition 4.8](#),

$$\mathbb{P}(\|(\mathbf{I} - \mathbf{v}_n(T)\mathbf{v}_n(T)^\top)\nabla^2 f(\mathbf{x}_n)\mathbf{v}_n(T)\|_2 < 2\epsilon + Mdl(0)^2) \geq 1 - \frac{10M^2d}{m_n\epsilon^2}.$$

Moreover, by choosing $m_n = O(n^p)$ with $p > 1$, the probability that

$$\|(\mathbf{I} - \mathbf{v}_n(T)\mathbf{v}_n(T)^\top)\nabla^2 f(\mathbf{x}_n)\mathbf{v}_n(T)\|_2 < 2\epsilon + Mdl(0)^2 \text{ for every } n \in \mathbb{N}$$

holds is bounded from below by $\prod_{n=1}^{\infty} (1 - O(\frac{1}{n^p})) > 0$. \square

4.4. Convergence of the outer derivative-free saddle search algorithm.

From [Proposition 4.6](#), the output $\{\tilde{\mathbf{v}}_i\}_1^k$, of [Algorithm 3.1](#) can almost surely approximate the unstable directions of both $f(\mathbf{x})$ (i.e., $\{\mathbf{v}_i\}_1^k$) and $f_l(\mathbf{x})$ (i.e., $\{\mathbf{v}_{l,i}\}_1^k$) with arbitrarily small error in a finite number of iterations if l is small enough. It is worth noting that $\mathbf{x}(n)$ is generally close to $\mathbf{x}(n+1)$ so that $\{\mathbf{v}_i(n)\}_1^k$ serves as a good initial condition for $\{\mathbf{v}_i(n+1)\}_1^k$, thus, a relatively small $n_{\mathbf{v}}^{max}$ (e.g., $n_{\mathbf{v}}^{max} = 10$) is often sufficient to obtain $\mathbf{v}(n+1)$ with satisfactory accuracy in practice. Thus, rather than imposing the stopping criterion in [Corollary 4.9](#), which requires many function evaluations, we recommend in practice simply imposing the maximum number of iterations $n_{\mathbf{v}}^{max}$ to reduce the computational cost. Nevertheless, the stopping criterion in [Corollary 4.9](#) guarantees that, with positive probability, each inner eigenvector search returns a good output. In this subsection, we work under the condition that this event occurs, i.e., we assume that the vectors returned by the inner loop are sufficiently close to the unstable eigenvectors, as made precise in the following assumption.

ASSUMPTION 4.1. *There is a small parameter θ such that, at any n -th outer iteration,*

$$(4.5) \quad \theta > \frac{\sqrt{2k}Ml(n)^2d}{4\mu} > 0, \text{ and } (1 - \sqrt{\theta})\mu_{l(n)} - M\theta - 5M\sqrt{\theta} > 0$$

holds, where $\mu_{l(n)} = \mu - Ml(n)^2d/2$, and the following conditions hold almost surely,

$$(4.6) \quad \min(\|\tilde{V}(n)\tilde{V}(n)^\top - V(n)V(n)^\top\|_2^2, \|\tilde{V}(n)\tilde{V}(n)^\top - V_{l(n)}V_{l(n)}^\top\|_2^2) \leq \theta,$$

where $\tilde{V}(n)\tilde{V}(n)^\top = \sum_{i=1}^k \tilde{\mathbf{v}}_i(\mathbf{x}(n))\tilde{\mathbf{v}}_i(\mathbf{x}(n))^\top$ is the projection operator with respect to, respectively, the output of the [Algorithm 3.1](#) with $\mathbf{x} = \mathbf{x}(n)$. Likewise, the operators $V(n)V(n)^\top = \sum_{i=1}^k \mathbf{v}_i(\mathbf{x}(n))\mathbf{v}_i(\mathbf{x}(n))^\top$, $V_{l(n)}V_{l(n)}^\top = \sum_{i=1}^k \mathbf{v}_{l(n),i}(\mathbf{x}(n))\mathbf{v}_{l(n),i}(\mathbf{x}(n))^\top$ are projections with respect to the k eigenvectors corresponding to the k smallest eigenvalues of $\nabla^2 f(\mathbf{x}(n))$ and $\nabla^2 f_{l(n)}(\mathbf{x}(n))$.

THEOREM 4.10 (Decay $l(n)$ with decay step size $\alpha(n)$). *Suppose the [Assumption 3.1](#), [Assumption 3.2](#), [Assumption 3.3](#), [Assumption 3.4](#), and [Assumption 4.1](#) hold. If the initial point $\mathbf{x}(0)$ is sufficiently close to \mathbf{x}^* , and that $\sum_{n=0}^{\infty} \alpha(n)^2$ is sufficiently small (e.g., $\alpha(n) = \frac{\gamma}{(n+m)^p}$ with some $p \in (1/2, 1]$, and a large enough m), the following boundedness event occurs with a high probability,*

(4.7)

$$E^\infty = \{\mathbf{x}(n) \in U, \forall n\}, \quad U = \left\{ \mathbf{x}, \|\mathbf{x} - \mathbf{x}^*\|_2 \leq \min \left(\frac{(1 - \sqrt{\theta})\mu}{M} - \theta - 5\sqrt{\theta}, \delta \right) \right\}.$$

Conditioned on E^∞ , given any tolerance $\epsilon_{\mathbf{x}} > 0$, the [Algorithm 3.2](#) almost surely reaches the $\epsilon_{\mathbf{x}}$ -neighborhood of \mathbf{x}^* in a finite number of iterations.

Proof. The proof is given in the Appendix. Since $F(\mathbf{x}, \mathbf{r}, l)$ is a biased gradient estimator with a bias term of order $O(l^2)$ ([Lemma 3.3](#)), we can use the bound on the decaying $l(n)$ with the step size $\alpha(n)$ ([Assumption 3.2](#)) to control this biased error. \square

However, if $l(n)$, appearing as a denominator in $F(\mathbf{x}(n), \mathbf{r}(n), l(n))$, is too small, then $F(\mathbf{x}(n), \mathbf{r}(n), l(n))$ may be dominated by round-off error and fail to approximate the gradient. Thus, in the rest of the section, let us consider the case with a small enough but constant $l(n) \equiv l > 0$.

LEMMA 4.11. *Suppose the Assumption 3.1, Assumption 3.3, Assumption 3.4, Assumption 3.5, and Assumption 4.1 hold. If the initial point $\mathbf{x}(0)$ is sufficiently close to \mathbf{x}^* and $\sum_{n=0}^{\infty} \alpha(n)^2$ is sufficiently small, then, the boundedness event*

$$E_l^{\infty} = \{\mathbf{x}(n) \in U, \forall n\}, \quad U_l = \left\{ \mathbf{x}, \|\mathbf{x} - \mathbf{x}^*\|_2 \leq \min \left(\frac{(1 - \sqrt{\theta})\mu_l}{M} - \theta - 5\sqrt{\theta}, \delta \right) \right\}$$

occurs with a high probability. Conditioned on E_l^{∞} , given any tolerance $\epsilon_{\mathbf{x}} > 0$, the Algorithm 3.2 almost surely reaches the $\epsilon_{\mathbf{x}}$ -neighborhood of \mathbf{x}_l^* in a finite number of iterations.

Proof. Note that $F(\mathbf{x}(n), \mathbf{r}(n), l)$ is the unbiased gradient estimator of $f_l(\mathbf{x}(n))$. Therefore, the proof then follows the same steps as in that of Theorem 4.10 by assuming that the biased error is zero. \square

Lemma 4.11 shows that the iteration points have a large probability to converge to \mathbf{x}_l^* . It is therefore natural to estimate the distance between \mathbf{x}_l^* and the target saddle point \mathbf{x}^* . From (3.8), the difference between the gradients and Hessians of $\nabla f(\mathbf{x})$ and $\nabla f_l(\mathbf{x})$ are of $O(l^2)$. Consequently, we can expect that their zeros, namely \mathbf{x}^* and \mathbf{x}_l^* , are also separated by a distance of $O(l^2)$, as made precise in Lemma 4.12.

LEMMA 4.12. *Suppose Assumption 3.3 and Assumption 3.4 hold. If $l > 0$ is a sufficiently small parameter such that $\mu_l > 0$, $\frac{Ml^2d}{\mu_l} = \delta_l \leq \frac{\delta}{2}$, $\frac{M\delta_l}{\mu_l} \leq \frac{1}{2}$. Then, there exists an $\mathbf{x}_l^* \in \{\mathbf{x}, \|\mathbf{x} - \mathbf{x}^*\|_2 \leq \delta_l\}$ which is an index- k saddle point of f_l , such that*

$$(4.8) \quad \|\mathbf{x}_l^* - \mathbf{x}^*\|_2^2 \leq \delta_l^2 = \left(\frac{Ml^2d}{\mu_l} \right)^2 = O(l^4).$$

Proof. We borrow the technique described in [24, Section 5.4] to estimate the distance between the zeros of two functions whose gradients and Hessians are close. Define the Newton iteration map as $T(\mathbf{x}) = \mathbf{x} - (\nabla^2 f_l(\mathbf{x}^*))^{-1} \nabla f_l(\mathbf{x})$. For $\mathbf{x}, \mathbf{y} \in \{\mathbf{x}, \|\mathbf{x} - \mathbf{x}^*\|_2 \leq \delta_l\}$, we have

$$\begin{aligned} \|T(\mathbf{x}) - T(\mathbf{y})\|_2 &= \|(\mathbf{x} - \mathbf{y}) - (\nabla^2 f_l(\mathbf{x}^*))^{-1} (\nabla f_l(\mathbf{x}) - \nabla f_l(\mathbf{y}))\|_2 \\ &= \left\| \left[(\nabla^2 f_l(\mathbf{x}^*))^{-1} \int_0^1 (\nabla^2 f_l(\mathbf{x}^*) - \nabla^2 f_l(\mathbf{y} + t(\mathbf{x} - \mathbf{y}))) dt \right] (\mathbf{x} - \mathbf{y}) \right\|_2 \\ &\leq \frac{M\delta_l}{\mu_l} \|\mathbf{x} - \mathbf{y}\|_2 \leq \frac{\|\mathbf{x} - \mathbf{y}\|_2}{2}. \end{aligned}$$

From (3.8), we have $\|\nabla f_l(\mathbf{x}^*)\|_2 = \|\nabla f_l(\mathbf{x}^*) - \nabla f(\mathbf{x}^*)\|_2 \leq \frac{Ml^2d}{2}$; from (3.9), we have that $\|(\nabla^2 f_l(\mathbf{x}^*))^{-1}\|_2 \leq \frac{1}{\mu_l}$. Thus, if $\mathbf{x} \in \{\mathbf{x}, \|\mathbf{x} - \mathbf{x}^*\|_2 \leq \delta_l\}$,

$$\begin{aligned} \|T(\mathbf{x}) - \mathbf{x}^*\|_2 &= \|\mathbf{x} - (\nabla^2 f_l(\mathbf{x}^*))^{-1} \nabla f_l(\mathbf{x}) - \mathbf{x}^*\|_2 \\ &\leq \underbrace{\|\mathbf{x} - (\nabla^2 f_l(\mathbf{x}^*))^{-1} (\nabla f_l(\mathbf{x}) - \nabla f_l(\mathbf{x}^*)) - \mathbf{x}^*\|_2}_{=\|T(\mathbf{x}) - T(\mathbf{x}^*)\|_2} + \underbrace{\|(\nabla^2 f_l(\mathbf{x}^*))^{-1} \nabla f_l(\mathbf{x}^*)\|_2}_{\leq \|(\nabla^2 f_l(\mathbf{x}^*))^{-1}\|_2 \|\nabla f_l(\mathbf{x}^*)\|_2} \\ &\leq \frac{1}{2} \|\mathbf{x} - \mathbf{x}^*\|_2 + \frac{Ml^2d}{2\mu_l} \leq \frac{\delta_l}{2} + \frac{\delta_l}{2} = \delta_l, \end{aligned}$$

which means $T(\mathbf{x})$ is a contraction mapping in $\{\mathbf{x}, \|\mathbf{x} - \mathbf{x}^*\|_2 \leq \delta_l\}$. According to the Banach fixed point theorem, there exists an $\mathbf{x}_l^* \in \{\mathbf{x}, \|\mathbf{x} - \mathbf{x}^*\|_2 \leq \delta_l\}$ such that $T(\mathbf{x}_l^*) = \mathbf{x}_l^*$, which means \mathbf{x}_l^* is a critical point of $f_l(\mathbf{x})$. Since $\mathbf{x}_l^* \in \{\mathbf{x}, \|\mathbf{x} - \mathbf{x}^*\|_2 \leq \delta_l\} \subset \{\mathbf{x}, \|\mathbf{x} - \mathbf{x}^*\|_2 \leq \delta\}$, we have (4.8). From (3.9), we know that \mathbf{x}_l^* is an index- k saddle point of $f_l(\mathbf{x})$. \square

By Lemma 4.11 and Lemma 4.12, we can directly have the following theorem.

THEOREM 4.13 (Constant $l(n) \equiv l$ with decay step size $\alpha(n)$). *With the same conditions and assumptions given in Lemma 4.11 and Lemma 4.12, the output of Algorithm 3.2 satisfies $\|\mathbf{x}^{\text{end}} - \mathbf{x}^*\|_2 \leq \|\mathbf{x}^{\text{end}} - \mathbf{x}_l^*\|_2 + \|\mathbf{x}^* - \mathbf{x}_l^*\|_2 < \epsilon_{\mathbf{x}} + \frac{Ml^2d}{\mu_l}$, which means that as the number of iterations tends to infinity, so that the tolerance $\epsilon_{\mathbf{x}}$ approaches zero, the distance between the output \mathbf{x}^{end} and the target saddle point \mathbf{x}^* , i.e. $\|\mathbf{x}^{\text{end}} - \mathbf{x}^*\|_2^2$, is almost surely no greater than a small constant $\left(\frac{Ml^2d}{\mu_l}\right)^2 = O(l^4)$.*

Although the above discussions theoretically show that the iterations of Algorithm 3.2 converge almost surely to \mathbf{x}^* (with a decaying $l(n)$) or to \mathbf{x}_l^* (with a constant $l(n)$) conditioned on the boundedness event, the decaying step size defined in Assumption 3.1 leads to a sublinear convergence rate. From Lemma 3.3, as the iteration point approaches the saddle point, $\|\nabla f(\mathbf{x})\|_2$ vanishes and the variance of $F(\mathbf{x}, \mathbf{r}, l)$ nearly goes to zero. This phenomenon is known as variance reduction [23, 7], which is commonly used in stochastic gradient methods to accelerate the convergence. When this occurs, it is usually unnecessary to use a decay step size to control the stochastic noise, allowing the use of a constant step size to achieve a linear convergence rate.

THEOREM 4.14 (Constant $l(n) \equiv l$ with constant step size $\alpha(n) \equiv \alpha$). *Suppose the Assumption 3.3, Assumption 3.4, and Assumption 4.1 hold. Let us pick a step size $\alpha(n) \equiv \alpha > 0$ sufficiently small such that $0 < \alpha < \frac{(1-\sqrt{\theta})\mu-M\theta-5M\sqrt{\theta}}{(2d+4)M^2+1}$. Then, provided that the boundedness event E^∞ occurs with a positive probability, the iterations generated by Algorithm 3.2 approach a neighborhood of \mathbf{x}^* with radius $O(l^2/\sqrt{\alpha})$, at a linear decay rate determined by a constant $0 < \sigma < 1$, i.e.,*

$$(4.9) \quad \mathbb{E}[\|\mathbf{x}(n) - \mathbf{x}^*\|_2^2 | E^\infty] \leq O(\sigma^n + l^4/\alpha).$$

Proof. Define the events $E^n = \{\mathbf{x}(i) \in U, i = 1, 2, \dots, n\}$ and corresponding indicator function $\mathbf{1}_{E^n}$. From Lemma 6.1 in the Appendix and Lemma 3.3, we have

$$\begin{aligned} \mathbb{E}[\mathbf{1}_{E^{n+1}} \|\mathbf{x}(n+1) - \mathbf{x}^*\|_2^2] &\leq \mathbb{E}[\mathbf{1}_{E^n} \|\mathbf{x}(n+1) - \mathbf{x}^*\|_2^2] \\ &\leq \mathbb{E}[\mathbb{E}[\mathbf{1}_{E^n} \|\mathbf{x}(n+1) - \mathbf{x}^*\|_2^2 | \mathcal{F}(n)]] \\ &\leq (1 - \alpha((1 - \sqrt{\theta})\mu - M\theta - 5M\sqrt{\theta})) \mathbb{E}[\mathbf{1}_{E^n} \|\mathbf{x}(n) - \mathbf{x}^*\|_2^2] \\ &\quad + \alpha M d l^2 \mathbb{E}[\mathbf{1}_{E^n} \|\mathbf{x}(n) - \mathbf{x}^*\|_2] \\ &\quad + \alpha^2 ((2d+4) \mathbb{E}[\mathbf{1}_{E^n} \|\nabla f(\mathbf{x})\|_2^2] + M^2 l^4 d(d+2)(d+4)(d+6)/18). \end{aligned}$$

From Young's inequality and Jensen's inequality, we have

$$\begin{aligned} \alpha M d l^2 \mathbb{E}[\mathbf{1}_{E^n} \|\mathbf{x}(n) - \mathbf{x}^*\|_2] &\leq \alpha^2 (\mathbb{E}[\mathbf{1}_{E^n} \|\mathbf{x}(n) - \mathbf{x}^*\|_2])^2 + M^2 d^2 l^4 / 4 \\ &\leq \alpha^2 \mathbb{E}[\mathbf{1}_{E^n} \|\mathbf{x}(n) - \mathbf{x}^*\|_2^2] + M^2 d^2 l^4 / 4. \end{aligned}$$

Note that $\mathbf{1}_{E^n} \|\nabla f(\mathbf{x}(n))\|_2^2 \leq \mathbf{1}_{E^n} M^2 \|\mathbf{x}(n) - \mathbf{x}^*\|_2^2$. Then, we get

$$\mathbb{E}[\mathbf{1}_{E^{n+1}} \|\mathbf{x}(n+1) - \mathbf{x}^*\|_2^2] \leq \sigma \mathbb{E}[\mathbf{1}_{E^n} \|\mathbf{x}(n) - \mathbf{x}^*\|_2^2] + C_4,$$

where $\sigma = \sigma(\alpha, \theta, \mu, M, d) = 1 - \alpha((1 - \sqrt{\theta})\mu - M\theta - 5M\sqrt{\theta}) + \alpha^2(2d + 4)M^2 + \alpha^2$ and $C_4 = \frac{M^2d^2l^4}{4} + \frac{\alpha^2M^2l^4d(d+2)(d+4)(d+6)}{18} = O(l^4)$. By telescoping, we get

$$\mathbb{E}[\mathbf{1}_{E^n} \|\mathbf{x}(n) - \mathbf{x}^*\|_2^2] \leq \sigma^n \|\mathbf{x}(0) - \mathbf{x}^*\|_2^2 + C_4 \sum_{i=0}^{n-1} \sigma^i \leq \sigma^n \|\mathbf{x}(0) - \mathbf{x}^*\|_2^2 + \frac{C_4}{1 - \sigma}.$$

Since $C_4 = O(l^4)$ and $1 - \sigma = O(\alpha)$, this completes the proof. \square

From (4.9), we can expect that the performance of [Algorithm 3.2](#) initially exhibits a linear convergence rate σ^n , and then levels off at a small error of $O(l^4/\alpha)$, which leads to the plateau error as commonly referred to in optimization.

Remark 4.15. The numerical tests in [Section 5](#) indicate that the boundedness assumption in [Theorem 4.14](#) indeed holds. If suitable global information of the objective function is known, the boundedness assumption can be removed. For instance, if the eigenvalues of $\nabla^2 f(\mathbf{x})$ satisfy (3.7) and

$$\|\nabla^2 f(\mathbf{x}) - \nabla^2 f(\mathbf{y})\|_2 \leq C_5 < (1 - \sqrt{\theta})\mu - M\theta - 5M\sqrt{\theta}, \forall \mathbf{x}, \mathbf{y} \in \mathbb{R}^d,$$

the attraction basin of the saddle-search algorithm can be proved to be the entire space \mathbb{R}^d . Suppose both α and θ are sufficiently small, then $\sigma \approx 1 - \alpha\mu$. Thus, a larger α not only accelerates the error decay but also reduces the plateau error of the order $O(l^4/\alpha)$, see the numerical experiments presented in [Subsection 5.1](#) for further illustrations of this point. Therefore, [Theorem 4.14](#) suggests choosing the step size α as large as possible while maintaining numerical stability.

5. Numerical experiments. In this section, we present a series of numerical examples to demonstrate the practical applicability and the convergence rate of the algorithm, as well as how the plateau error depends on l and α .

Note that for $\mathbf{x}(n)$ near a strict saddle point \mathbf{x}^* , we have

$$\mu^2 \|\mathbf{x}(n) - \mathbf{x}^*\|_2^2 \leq \|\nabla f(\mathbf{x}(n))\|_2^2 = \|\nabla f(\mathbf{x}(n)) - \nabla f(\mathbf{x}^*)\|_2^2 \leq M^2 \|\mathbf{x}(n) - \mathbf{x}^*\|_2^2.$$

Thus, both $\|\mathbf{x}(n) - \mathbf{x}^*\|_2^2$ and $\|\nabla f(\mathbf{x}(n))\|_2^2$ can measure the error.

5.1. Müller-Brown potential. This numerical example illustrates the practicality of the proposed derivative-free saddle-search algorithm and verifies the predicted order of the plateau error established in the theoretical analysis. The Müller-Brown (MB) potential is a two-dimensional function in theoretical chemistry that describes a system with multiple local minima and saddle points, serving as a standard benchmark to test saddle-search algorithms. The MB potential is given by [4]

$$E(x, y) = \sum_{i=1}^4 A_i e^{a_i(x - \bar{x}_i)^2 + b_i(x - \bar{x}_i)(y - \bar{y}_i) + c_i(y - \bar{y}_i)^2},$$

where $A = [-200, -100, -170, 15]$, $a = [-1, -1, -6.5, 0.7]$, $b = [0, 0, 11, 0.6]$, $c = [-10, -10, -6.5, 0.7]$, $\bar{x} = [1, 0, -0.5, -1]$, and $\bar{y} = [0, 0.5, 1.5, 1]$. We show the contour plot of the MB potential in [Figure 2\(a\)](#) with two local minimizers (the reactant and product) and one index-1 saddle point (transition state) connecting two minimizers.

We set the initial condition to $\mathbf{x}(0) = (0, 1)^\top$, and compute the error versus the iteration number for $l = 0.001$ ([Figure 2\(b\)](#)) and $l = 0.0001$ ([Figure 2\(c\)](#)), respectively. The results show that at the early stage of the iterations, the error decreases at an

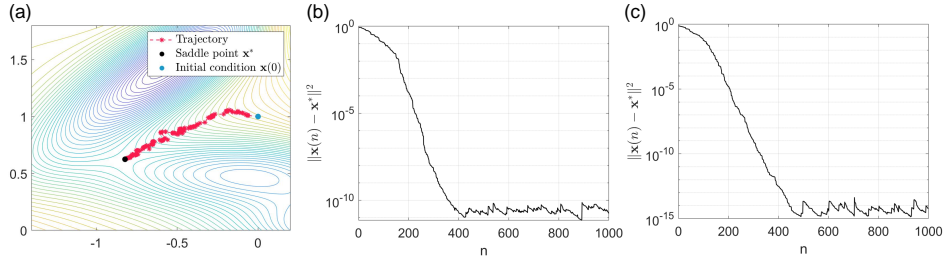


FIG. 2. Contour plot of MB potential and iteration points (a) of one-time run of [Algorithm 3.2](#). Error plots of the iteration points with (b) $l = 0.001$, $\alpha_x \equiv 0.0001$, $n_x^{max} = 1000$, $n_v^{max} = 100$, $\alpha_v \equiv 0.0002$ and (c) $l = 0.0001$, $\alpha_x \equiv 0.0001$, $n_x^{max} = 1000$, $n_v^{max} = 100$, $\alpha_v \equiv 0.0002/d$.

exponential rate, and eventually levels off at a small plateau error, which is consistent with [Theorem 4.14](#). Moreover, as l decreases from 0.001 to 0.0001, the plateau error decreases from 10^{-11} to 10^{-15} , which aligns with the $O(l^4)$ error predicted by both [Theorem 4.13](#) and [Theorem 4.14](#). To further verify the $O(l^4/\alpha)$ plateau error in [Theorem 4.14](#), we examine the plateau error for different difference lengths l and step sizes α in [Table 1](#). The plateau error is calculated as the average of the minimum errors over 100 runs, defined by $\frac{1}{100} \sum_{i=1}^{100} \min_n \|x^i(n) - x^*\|_2^2$. With respect to l , the rate of decay of the plateau error is approximately $O(l^4)$. Regarding α , when α increases from 0.0001 to 0.0002, the plateau error roughly halves. The numerical tests in [Table 1](#) are consistent with the $O(l^4/\alpha)$ scaling.

TABLE 1

Plateau error is computed as the mean of the minimum errors across $k = 100$ runs, defined by $\frac{1}{k} \sum_{i=1}^k \min_n \|x^i(n) - x^*\|_2^2$, with $n_x^{max} = 1000$, $n_v^{max} = 100$, $\alpha_v \equiv 0.0002$, $l(n) \equiv 0.001$.

l	$\alpha = 0.0001$		$\alpha = 0.0002$	
	Plateau error	Order of vanishing	Plateau error	Order of vanishing
2^{-8}	2.71E-09		1.28E-09	
2^{-9}	1.58E-10	4.28	7.73E-11	4.15
2^{-10}	1.02E-11	3.89	4.84E-12	3.99
2^{-11}	6.40E-13	3.97	2.96E-13	4.09
2^{-12}	3.87E-14	4.14	2.02E-14	3.66

5.2. Implicitly defined objective function. This numerical example demonstrates that our method is applicable to implicitly defined objective functions, whose gradients and Hessians are difficult to obtain explicitly. Such problems arise, for instance, in hyperparameter optimization [14] and in self-consistent field theory in materials science [15], where the objective function is typically defined through a minimization problem. For brevity and clearer visualization, we consider the following two-dimensional implicit function:

$$(5.1) \quad f(x, y) = \min_{\mathbf{z}} g(x, y, \mathbf{z}) = \min_{\mathbf{z}} (x - z_1)^2 + (y - z_2)^2 + \sin(z_1 z_2),$$

where each function evaluation is defined as the solution of an associated optimization problem. In [Figure 3\(a\)](#), we present the contour plot of the energy landscape, which indicates that $\mathbf{x}^* = (0, 0)$ is an index-1 saddle point of $f(x, y)$.

Actually, the Hessian of f is given by the implicit function theorem

$$\nabla^2 f(x, y) = \begin{pmatrix} g_{xx} & g_{xy} \\ g_{yx} & g_{yy} \end{pmatrix} - \begin{pmatrix} g_{xz_1} & g_{xz_2} \\ g_{yz_1} & g_{yz_2} \end{pmatrix} \begin{pmatrix} g_{z_1 z_1} & g_{z_1 z_2} \\ g_{z_2 z_1} & g_{z_2 z_2} \end{pmatrix}^{-1} \begin{pmatrix} g_{z_1 x} & g_{z_1 y} \\ g_{z_2 x} & g_{z_2 y} \end{pmatrix}.$$

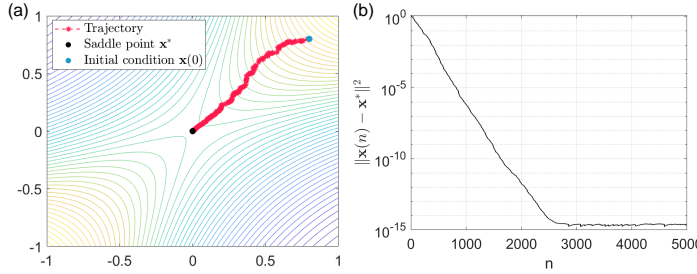


FIG. 3. (a) Contour plot of (5.1) and iteration points of one-time run of Algorithm 3.2. (b) Error plot with $l = 0.1$, $\alpha_{\mathbf{x}} \equiv 0.01$, $n_{\mathbf{x}}^{max} = 5000$, $n_{\mathbf{v}}^{max} = 100$, $\alpha_{\mathbf{v}} \equiv 0.0002/d$.

With all derivatives are evaluated at $(x, y, \mathbf{z}) = (0, 0, \mathbf{0})$, the Hessian of f at \mathbf{x}^* is

$$\nabla^2 f(0, 0) = \begin{bmatrix} 2 & 0 \\ 0 & 2 \end{bmatrix} - \begin{bmatrix} 8/3 & -4/3 \\ -4/3 & 8/3 \end{bmatrix} = \begin{bmatrix} -2/3 & 4/3 \\ 4/3 & -2/3 \end{bmatrix},$$

whose eigenvalues are $\lambda_1 = 2/3, \lambda_2 = -2$, showing that the origin is an index-1 saddle point of $f(x, y)$. In Figure 3(b), we plot the error versus the iteration number, showing that the iterates approach the saddle point with a linear convergence rate before leveling off at a small plateau error.

5.3. Modified Rosenbrock function. The following numerical experiments demonstrate that the algorithm can be applied to locate the high-index saddle point of the high-dimensional models, show the efficiency of the Hessian-vector product approximation compared with the Hessian approximation, and show that the zeroth-order algorithm also encounters slow convergence rates on ill-conditioned problems, similar to the typical gradient-based algorithms. The Rosenbrock function [41], also known as the banana function, features a narrow and curved valley with a flat energy landscape around the minimum. It is a classical benchmark for optimization algorithms due to its challenging geometry, which makes convergence to the global minimum difficult. To adapt the Rosenbrock example for saddle-point computation, we modify it by adding extra quadratic arctangent terms [48], yielding

$$f(\mathbf{x}) = \sum_{i=1}^{d-1} 100(x_{i+1} - x_i^2)^2 + (1 - x_i)^2 + \sum_{i=1}^d s_i \arctan^2(x_i - 1),$$

where $\{s_i\}_1^d$ are the parameters introduced to tune the index of the critical point $\mathbf{x}^* = (1, \dots, 1)^\top$. For example, when $d = 2, s_1 = -50, s_2 = 1$, \mathbf{x}^* is an index-1 saddle point, and the condition number $Cond(\nabla^2 f(\mathbf{x}^*)) \approx 47$. The energy landscape of the modified Rosenbrock function, shown in Figure 4(a), illustrates that the energy landscape near \mathbf{x}^* is relatively flat along the unstable direction. The convergence rate largely depends on the condition number of $\nabla^2 f(\mathbf{x}^*)$. According to Theorem 4.14, the error decays approximately as $\sigma^n \approx (1 - \alpha\mu)^n$. For numerical stability, the step size α should be smaller than $2/M$, which yields an error decay rate on the order of $(1 - 2/Cond(\nabla^2 f(\mathbf{x}^*)))^n$. It can be further observed from the iteration trajectory in Figure 4(a) that the iteration points tend to converge more rapidly along the steep directions, while moving slowly along the eigenvector corresponding to the smallest absolute eigenvalue. It is reflected in Figure 4(b) that the error decreases rapidly at the beginning of the iteration (along the steep directions), but slows down in the later stage (along the flat directions).

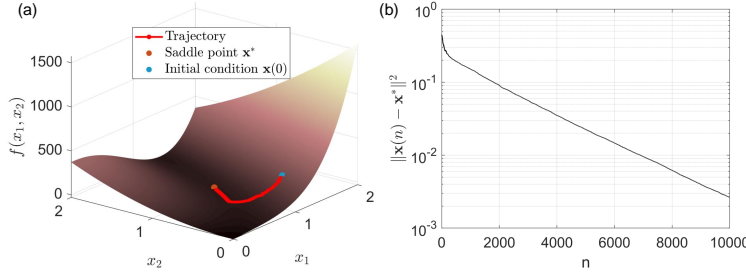


FIG. 4. (a) Energy landscape of the 2D Rosenbrock function and iteration points of one-time run of Algorithm 3.2. (b) Error plot of the iteration points of Algorithm 3.2 with $l = 0.0001$, $\alpha_{\mathbf{x}} \equiv 0.00001$, $n_{\mathbf{x}}^{max} = 10000$, $n_{\mathbf{v}}^{max} = 100$, $\alpha_{\mathbf{v}} \equiv 0.0002/d$.

We then examine the advantage of variance reduction when using the Hessian-vector approximation $H_{\mathbf{v}}$, as compared with the full Hessian approximation \mathbf{H} , in the eigenvector search. We search for the smallest eigenvalue and its corresponding eigenvector of $\nabla^2 f(\mathbf{x}^* + 0.5\mathbf{r})$, where \mathbf{r} is drawn from the standard normal distribution, and plot the resulting error in Figure 5(a). When the dimension is low, i.e., $d = 3$, both the Hessian approximation and the Hessian-vector approximation perform well. However, for $d = 100$, the variance of the Hessian approximation \mathbf{H} reaches the order of 10^8 , whereas that of the Hessian-vector approximation is only about 10^2 . As a result, the eigenvector search using the Hessian approximation becomes unstable and fails to converge to the true eigenvector \mathbf{v}^* , while the Hessian-vector approximation still performs well. Although thousands of iterations are required to obtain an accurate output in Figure 5(a), in practice, using the approximate unstable directions of $\nabla^2 f(\mathbf{x}(n))$ as the initial condition, we typically find the approximate unstable directions of $\nabla^2 f(\mathbf{x}(n+1))$ within tens of iterations in Algorithm 3.1. This is because $\mathbf{x}(n)$ is close to $\mathbf{x}(n+1)$, so the unstable directions of $\nabla^2 f(\mathbf{x}(n))$ (which we already have) serve as good initial conditions for those of $\nabla^2 f(\mathbf{x}(n+1))$.

We now consider a high-index saddle point in a high-dimensional setting. We choose $d = 1000$ and set $s_1 = s_2 = s_3 = -1000$, $s_i = 1$ for $i = 4, \dots, 1000$. Then, $\mathbf{x}^* = (1, \dots, 1)^\top$ is an index-3 saddle point with a large condition number, $Cond(\nabla^2 f(\mathbf{x}^*)) \approx 722$. In Figure 5(b), we plot the error versus iteration for both the zeroth-order algorithm and the deterministic algorithm. The error initially decays rapidly along the steepest directions and then slows down, similar to the behavior observed in Figure 4, but with a slower convergence rate due to the larger condition number of the Hessian. Hence, an interesting and important future direction could be to accelerate the convergence by introducing momentum to address the ill-conditioning. Importantly, the zeroth-order algorithm achieves a convergence rate comparable to that of the deterministic algorithm, without requiring gradient and Hessian evaluations.

5.4. Loss landscape of a neural network. In neural networks, the model parameters are sometimes hidden, and accessing gradient information is inadmissible, as in zeroth-order attacks [29]. In such cases, one typically has to resort to the derivative-free methods. We implement the derivative-free saddle-search algorithm on the loss landscape of the linear neural network to show that it also works for the degenerate high-index saddle point. Because of the overparameterization of neural networks, most critical points of the loss function are highly degenerate, i.e., the Hessian contains many zero eigenvalues. We consider a fully-connected linear neural

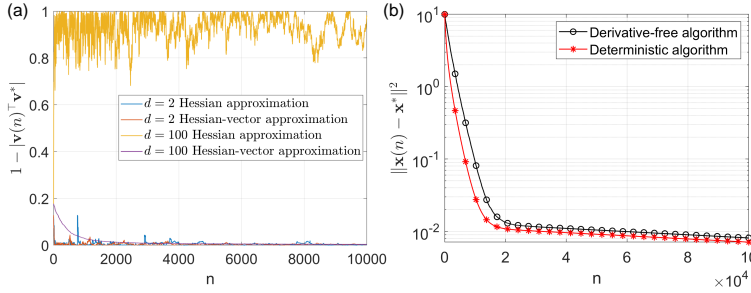


FIG. 5. (a) The error plots of the inner eigenvector search algorithm (Algorithm 3.1) with $d = 2$ and $d = 100$, using the Hessian approximation ($\mathbf{H}\mathbf{v}$) and the Hessian–vector approximation ($H\mathbf{v}$), respectively. The step size is chosen as $\alpha(n) = \frac{1}{d(10n+10000)}$. (b) Error plots of Algorithm 3.2 and the deterministic saddle-search algorithm in (2.2) applied to the modified Rosenbrock function with $d = 1000$, $l = 0.0001$, $\alpha_{\mathbf{x}} \equiv 0.000001$, $n_{\mathbf{x}}^{max} = 100000$, $n_{\mathbf{v}}^{max} = 100$, $\alpha_{\mathbf{v}} \equiv 0.0002/d$.

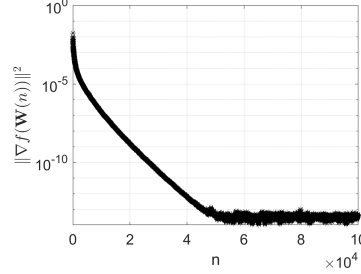


FIG. 6. Plots of the squared gradient norm $\|\nabla f(\mathbf{W}(n))\|_2^2$, where $\mathbf{W}(n)$ is the iteration points of Algorithm 3.2 with $\alpha_{\mathbf{x}} \equiv 0.01$, $l = 0.0001$, for the neural network loss function.

network $Net(\mathbf{W}, \mathbf{x}) = \mathbf{W}_H \mathbf{W}_{H-1} \cdots \mathbf{W}_2 \mathbf{W}_1 \mathbf{x}$ of depth H , with weight parameters $\mathbf{W}_{i+1} \in \mathbb{R}^{d_{i+1} \times d_i}$ for $d_0 = d_x$, $d_H = d_y$. The corresponding empirical loss f is defined by

$$f(\mathbf{W}) = \sum_{i=1}^N \|Net(\mathbf{W}, \mathbf{x}_i) - \mathbf{y}_i\|_2^2 = \|\mathbf{W}_H \mathbf{W}_{H-1} \cdots \mathbf{W}_2 \mathbf{W}_1 \mathbf{X} - \mathbf{Y}\|_F^2,$$

where $\mathbf{X} = [\mathbf{x}_1, \dots, \mathbf{x}_N]$, and $\mathbf{Y} = [\mathbf{y}_1, \dots, \mathbf{y}_N]$, with $\{(\mathbf{x}_i, \mathbf{y}_i)\}_{i=1}^N$ being the training data. If $d_i = d_0$, $1 \leq i \leq H-1$, then $\mathbf{W}^* = [\mathbf{W}_1^*, \dots, \mathbf{W}_H^*]$ is a saddle point where

$$\mathbf{W}_1^* = \begin{bmatrix} U_S^\top \Sigma_{YX} \Sigma_{XX}^{-1} \\ \mathbf{0} \end{bmatrix}, \mathbf{W}_h^* = \mathbf{I}_{d_0} \text{ for } 2 \leq h \leq H-1, \text{ and } \mathbf{W}_H^* = [\mathbf{U}_S, \mathbf{0}],$$

and \mathcal{S} is an index subset of $\{1, 2, \dots, r_{\max}\}$ for $r_{\max} = \min\{d_0, \dots, d_H\}$, $\Sigma_{XX} = XX^\top$, $\Sigma_{YX} = YX^\top$, $\Sigma = \Sigma_{YX} \Sigma_{XX}^{-1} \Sigma_{YX}^\top$, and U satisfies $\Sigma = U \Lambda U^\top$ with $\Lambda = \text{diag}(\lambda_1, \dots, \lambda_{d_y})$ [1, 31].

We set the depth $H = 5$, the input dimension $d_x = 10$, the output dimension $d_y = 4$, $d_i = 10$ for $1 \leq i \leq 4$, and the number of data points $N = 100$. Data points $(\mathbf{x}_i, \mathbf{y}_i)$ are sampled from the standard normal distributions. Under the current setting, \mathbf{W}^* is a degenerate saddle point with 16 negative eigenvalues and several zero eigenvalues. In Figure 6, we tested the derivative-free saddle-search algorithm, and the algorithm successfully locates the target saddle point, with a linear convergence rate. The error still levels off at a small plateau value, which is about 10^{-14} , and this plateau error can be further reduced by decreasing l .

6. Conclusion and discussion. This work focuses on the development and numerical analysis of a derivative-free algorithm for saddle point search, which requires only function evaluations. The proposed derivative-free saddle-search algorithm consists of two main components: an inner eigenvector-search step and an outer saddle-search step. For the inner eigenvector-search step, we adopt a zeroth-order Hessian-vector approximation to eliminate the curse of dimensionality, and prove that it almost surely identifies approximate unstable directions of both $\nabla^2 f(\mathbf{x})$ and $\nabla^2 f_l(\mathbf{x})$ within a finite number of iterations. Using these approximate unstable directions, we further prove that the outer derivative-free saddle-search step can identify the saddle point \mathbf{x}^* under a decaying difference length $l(n)$ and step size $\alpha(n)$. With a constant difference length and decay step size, the outer iteration almost surely converges to \mathbf{x}_l^* , which is a saddle point of the Gaussian smoothed function and is $O(l^2)$ -close to \mathbf{x}^* . Moreover, under a boundedness assumption, we establish that with both constant difference length and constant step size, the iterates approach a neighborhood of \mathbf{x}^* at a linear convergence rate, and the radius of this neighborhood is $O(l^2/\sqrt{\alpha})$. These results demonstrate that when the difference length l is sufficiently small, the algorithm output can closely approximate the target saddle point, which is further confirmed in our numerical experiments.

This study opens several potential directions for further exploration. The performance of both the derivative-free eigenvector-search algorithm and the derivative-free saddle-search algorithm can be improved by incorporating certain techniques from derivative-free optimization methods. For example, the gradient of the Gaussian-smoothed function is difficult to estimate because it involves a d -dimensional integral; a directional Gaussian smoothing may provide a more efficient way to design the gradient estimator [45]. Moreover, by introducing the error-correction term, the variance of the estimator can be reduced [29, 22], thereby accelerating convergence as stated in (4.3). In addition, incorporating momentum into the algorithm, as in [5], may accelerate convergence, especially when the energy landscape near the saddle point \mathbf{x}^* is flat (or $\nabla^2 f(\mathbf{x}^*)$ is ill-conditioned), such as in the modified Rosenbrock function in Subsection 5.3. A possible theoretical challenge, however, lies in ensuring that the iterates remain within the neighborhood of the target saddle point, at least with positive probability. Overall, since the derivative-free saddle-search algorithm could be seen as a gradient-estimate method, it is reasonable to expect that many techniques developed for the derivative-free optimization methods could be applied to it as well. However, the additional difficulties arise from the intrinsically unstable nature of saddle points and the nonconvexity of the objective function.

A. Appendix.

A.1. Proof of Lemma 3.3.

Proof. Denote $\mathbf{r}^{\otimes i} = \underbrace{[\mathbf{r}, \dots, \mathbf{r}]}_{i \text{ times}} := \underbrace{\mathbf{r} \otimes \mathbf{r} \otimes \dots \otimes \mathbf{r}}_{i \text{ times}}$, for $i \geq 2$. We have

$$\nabla f_l(\mathbf{x}) = \mathbb{E}_{\mathbf{r}}[\nabla f(\mathbf{x} + l\mathbf{r})] = \nabla f(\mathbf{x}) + l^2 \mathbb{E}_{\mathbf{r}}[\nabla^3 f(\zeta_{1,l,\mathbf{r}})[\mathbf{r}, \mathbf{r}]]/2,$$

$$\nabla^2 f_l(\mathbf{x}) = \mathbb{E}_{\mathbf{r}}[\nabla^2 f(\mathbf{x} + l\mathbf{r})] = \nabla^2 f(\mathbf{x}) + l^2 \mathbb{E}_{\mathbf{r}}[\nabla^4 f(\zeta_{2,l,\mathbf{r}})[\mathbf{r}, \mathbf{r}]]/2,$$

from the Taylor expansion. Hence

$$\|\nabla f_l(\mathbf{x}) - \nabla f(\mathbf{x})\|_2 \leq Ml^2 d/2, \quad \|\nabla^2 f_l(\mathbf{x}) - \nabla^2 f(\mathbf{x})\|_2 \leq Ml^2 d/2.$$

To calculate the second-order moment of $F(\mathbf{x}, \mathbf{r}, l)$, we consider

$$f(\mathbf{x} \pm l\mathbf{r}) = f(\mathbf{x}) \pm l\nabla f(\mathbf{x})^\top \mathbf{r} + l^2 \mathbf{r}^\top \nabla^2 f(\mathbf{x}) \mathbf{r} + l^3 \nabla^3 f(\xi_{\pm})[\mathbf{r}, \mathbf{r}, \mathbf{r}]/6,$$

Then, $F(\mathbf{x}, \mathbf{r}, l) = (\nabla f(\mathbf{x})^\top \mathbf{r}) \mathbf{r} + M_2 \mathbf{r}$, where $|M_2| \leq \frac{l^2 M \|\mathbf{r}\|_2^3}{6}$. From Isserlis's theorem,

$$\begin{aligned} \mathbb{E}_{\mathbf{r}}(\|(\nabla f(\mathbf{x})^\top \mathbf{r}) \mathbf{r}\|^2) &= \sum_{i=1}^d \sum_{j=1}^d \sum_{k=1}^d \nabla f(\mathbf{x})_j \nabla f(\mathbf{x})_k \mathbb{E}(r_i r_i r_j r_k) = (d+2) \|\nabla f(\mathbf{x})\|^2, \\ \mathbb{E}_{\mathbf{r}}(\|F(\mathbf{x}, \mathbf{r}, l)\|^2) &\leq 2\mathbb{E}_{\mathbf{r}}(\|(\nabla f(\mathbf{x})^\top \mathbf{r}) \mathbf{r}\|_2^2) + M^2 l^4 \mathbb{E}_{\mathbf{r}}(\|\mathbf{r}\|^8)/18 \\ &\leq (2d+4) \|\nabla f(\mathbf{x})\|_2^2 + M^2 l^4 d(d+2)(d+4)(d+6)/18. \end{aligned}$$

For the Hessian approximation, we consider the following Taylor expansions,

$$f(\mathbf{x} \pm l\mathbf{r}) = f(\mathbf{x}) \pm l \nabla f(\mathbf{x})^\top \mathbf{r} + \frac{l^2}{2} \mathbf{r}^\top \nabla^2 f(\mathbf{x}) \mathbf{r} \pm \frac{l^3}{6} \nabla^3 f(\mathbf{x})[\mathbf{r}^{\otimes 3}] + \frac{l^4}{24} \nabla^4 f(\xi_{\pm})[\mathbf{r}^{\otimes 4}].$$

Then $\mathbf{H}(\mathbf{x}, \mathbf{r}, l) = \frac{(\mathbf{r}^\top \nabla^2 f(\mathbf{x}) \mathbf{r})(\mathbf{r} \mathbf{r}^\top - \mathbf{I})}{2} + M_3(\mathbf{r} \mathbf{r}^\top - \mathbf{I})$ with $|M_3| \leq \frac{l^2 M \|\mathbf{r}\|_2^4}{24}$. From

$$\begin{aligned} \mathbb{E}_{\mathbf{r}}[\|\mathbf{r}^\top \nabla^2 f(\mathbf{x}) \mathbf{r}(\mathbf{r} \mathbf{r}^\top - \mathbf{I})\|_2^2/4] &\leq \|\nabla^2 f(\mathbf{x})\|_2^2 (\mathbb{E}_{\mathbf{r}}[\|\mathbf{r}\|^8 + 2\|\mathbf{r}\|^6 + \|\mathbf{r}\|^4])/4 \\ &\leq d(d+2)(d^2 + 12d + 33)M^2/4, \end{aligned}$$

we have that

$$\begin{aligned} \mathbb{E}_{\mathbf{r}}[\|\mathbf{H}(\mathbf{x}, \mathbf{r}, l)\|_2^2] &\leq 2\mathbb{E}_{\mathbf{r}}[\|\mathbf{r}^\top \nabla^2 f(\mathbf{x}) \mathbf{r}(\mathbf{r} \mathbf{r}^\top - \mathbf{I})\|_2^2/4] + 2\mathbb{E}_{\mathbf{r}}[M_3^2 \|\mathbf{r} \mathbf{r}^\top - \mathbf{I}\|_2^2] \\ &\leq d(d+2)(d^2 + 12d + 33)M^2/2 \\ &\quad + M^2 l^4 d(d+2)(d+4)(d+6)(d^2 + 20d + 97)/288. \end{aligned}$$

A.2. Proof of Lemma 4.5.

Proof.

$$\begin{aligned} \mathbb{E}_{\mathbf{r}}[H_{\mathbf{v}}] &= \frac{\mathbb{E}_{\mathbf{r}}[F(\mathbf{x} + l\mathbf{v}, \mathbf{r}, l)] - \mathbb{E}_{\mathbf{r}}[F(\mathbf{x} - l\mathbf{v}, \mathbf{r}, l)]}{2l} = \frac{\nabla f_l(\mathbf{x} + l\mathbf{v}) - \nabla f_l(\mathbf{x} - l\mathbf{v})}{2l} \\ &= \nabla^2 f_l(\mathbf{x}) \mathbf{v} + \frac{l^2}{12} (\nabla^4 f_l(\xi_+) - \nabla^4 f_l(\xi_-))[\mathbf{v}, \mathbf{v}, \mathbf{v}], \end{aligned}$$

$$\|\mathbb{E}_{\mathbf{r}}[H_{\mathbf{v}}] - \nabla^2 f(\mathbf{x}) \mathbf{v}\|_2 \leq \|\nabla^2 f(\mathbf{x}) - \nabla^2 f_l(\mathbf{x})\|_2 + Ml^2/6 \leq Ml^2(d/2 + 6) \leq Ml^2 d.$$

By the Taylor expansions, we get

$$\begin{aligned} H_{\mathbf{v}} &= \frac{F(\mathbf{x} + l\mathbf{v}, \mathbf{r}, l) - F(\mathbf{x} - l\mathbf{v}, \mathbf{r}, l)}{2l} \\ &= \mathbf{r} \mathbf{r}^\top \nabla^2 f(\mathbf{x}) \mathbf{v} + \frac{l^2}{6} (\nabla^4 f(\mathbf{x})[\mathbf{v}, \mathbf{v}, \mathbf{v}, \mathbf{r}] + \nabla^4 f(\mathbf{x})[\mathbf{v}, \mathbf{r}, \mathbf{r}, \mathbf{r}]) \mathbf{r} + O(l^4). \end{aligned}$$

Thus, from the Cauchy–Schwarz inequality, we have that

$$\mathbb{E}_{\mathbf{r}}(\|H_{\mathbf{v}}\|_2^2) \leq M^2(4(d+2) + l^4 d(d+2)/9 + l^4 d(d+2)(d+4)(d+6)/9) + O(l^8 d^8).$$

A.3. Proof of Theorem 4.10.

LEMMA 6.1 (Proposition 4.15 of [42]). *Suppose the Assumption 3.3, Assumption 3.4 and Assumption 4.1 hold. Let a neighborhood U of \mathbf{x}^* be defined as in (4.7).*

If $\mathbf{x}(n) \in U$, we almost surely have

$$\begin{aligned} (6.1) \quad \|\mathbf{x}(n+1) - \mathbf{x}^*\|_2^2/2 &\leq (1 - \alpha(n)((1 - \sqrt{\theta})\mu - M\theta - 5M\sqrt{\theta})) \|\mathbf{x}(n) - \mathbf{x}^*\|_2^2/2 \\ &\quad + \alpha(n)\psi(n) + \frac{1}{2}\alpha(n)^2 \|F(\mathbf{x}(n), \mathbf{r}(n), l(n))\|_2^2, \end{aligned}$$

where $\psi(n) = -\langle (\mathbf{I} - 2\tilde{V}(n)\tilde{V}(n)^\top)(F(\mathbf{x}(n), \mathbf{r}(n), l(n)) - \nabla f(\mathbf{x}(n))), \mathbf{x}(n) - \mathbf{x}^* \rangle$.

LEMMA 6.2. Suppose the [Assumption 3.1](#), [Assumption 3.2](#), [Assumption 3.3](#), [Assumption 3.4](#), and [Assumption 4.1](#) hold. If we assume that the outer saddle-search algorithm is implemented with the step size satisfying that $\sum_{n=0}^{\infty} \alpha(n)^2$ is sufficiently small (e.g. $\alpha(n) = \frac{\gamma}{(n+m)^p}$ with a large enough m and $p \in (1/2, 1]$). Set ϵ and U_0 as (6.2)

$$4\epsilon + 2\sqrt{\epsilon} = \min \left(\frac{(1 - \sqrt{\theta})\mu}{M} - \theta - 5\sqrt{\theta}, \delta \right)^2, U_0 = \left\{ \mathbf{x}, \|\mathbf{x} - \mathbf{x}^*\|_2 \leq \sqrt{2\epsilon} \right\} \subset U,$$

where U is defined in (4.7). Then, for $\mathbf{x}(n)$ generated by the saddle-search algorithm with an initial condition $\mathbf{x}(0) \in U_0$, the event E^∞ defined in (4.7) occurs with a positive probability. In a particular case, if the saddle-search algorithm is run with a step-size schedule of the form $\alpha(n) = \frac{\gamma}{(n+m)^p}, p \in (1/2, 1]$ and large enough m , then $\mathbb{P}(E^\infty | \mathbf{x}(0) \in U_0) > 1 - \epsilon_{E^\infty}$, and $1 - \epsilon_{E^\infty} \rightarrow 1$ as $m \rightarrow \infty$.

Proof. Since [Lemma 6.1](#) is analogous to [32, Proposition D.1], which constitutes a key step in establishing the positive probability of the event E^∞ , the proof proceeds along the same lines as [32, Theorem 4]. Thus, we omit the details and give the main steps. The places different from the original proof are: (i) the gradient term appears as $(\mathbf{I} - 2\tilde{V}(n)\tilde{V}(n)^\top)\nabla f$ rather than ∇f , which does not affect its L^2 norm; (ii) the upper bound of $\|\nabla f(\mathbf{x})\|_2$, $G = \max_{\mathbf{x} \in U} \|\nabla f(\mathbf{x})\|_2$, is not global but restricted to $\mathbf{x} \in U$, which does not alter the proof steps; and (iii) $\psi(n) = -\langle (\mathbf{I} - 2\tilde{V}(n)\tilde{V}(n)^\top)(F(\mathbf{x}(n), \mathbf{r}(n), l(n)) - \nabla f(\mathbf{x}(n))), \mathbf{x}(n) - \mathbf{x}^* \rangle$ is not a martingale sequence with zero expectation, and we need to estimate the error induced by the biased zeroth-order gradient estimator.

By [Lemma 6.1](#), the distance between the iteration point and saddle point almost surely grows at most by $\alpha(n)\psi(n) + \frac{1}{2}\alpha(n)^2\|F(\mathbf{x}(n), \mathbf{r}(n), l(n))\|_2^2$ at each step. Define the cumulative mean square error

$$R^n = \left(\sum_{i=0}^n \alpha(i)\psi(i) \right)^2 + \sum_{i=0}^n \frac{1}{2}\alpha(i)^2\|F(\mathbf{x}(i), \mathbf{r}(i), l(i))\|_2^2.$$

Set ϵ and $U_0 \subset U$ as in (6.2). Then, if $\mathbf{x}(0) \in U_0$, and the cumulative mean square error $R^n < \epsilon$, we almost surely have that

$$\begin{aligned} \|\mathbf{x}(n+1) - \mathbf{x}^*\|_2^2 &\leq \|\mathbf{x}(0) - \mathbf{x}^*\|_2^2 + 2 \sum_{i=0}^n \alpha(i)\psi(i) + \sum_{i=0}^n \alpha(i)^2\|F(\mathbf{x}(i), \mathbf{r}(i), l(i))\|_2^2 \\ &\leq 2\epsilon + 2\sqrt{\epsilon} + 2\epsilon = 4\epsilon + 2\sqrt{\epsilon}, \end{aligned}$$

i.e., $\mathbf{x}(n+1) \in U$. Define the small error event $J^n = \{R_k \leq \epsilon, k = 1, \dots, n\}$, and the boundedness event $E^n = \{\mathbf{x}(i) \in U, i = 1, 2, \dots, n\}$. By [32, Lemma D.2.], we have $E^{n+1} \subseteq E^n, J^{n+1} \subseteq J^n, J^{n-1} \subseteq E^n$, which means that a small error ensures the occurrence of the boundedness event. Different from [32, Lemma D.2.] where an unbiased stochastic gradient is used so that $\psi(n)$ is a martingale with zero expectation, $\psi(n) = -\langle (\mathbf{I} - 2\tilde{V}(n)\tilde{V}(n)^\top)(F(\mathbf{x}(n), \mathbf{r}(n), l(n)) - \nabla f(\mathbf{x}(n))), \mathbf{x}(n) - \mathbf{x}^* \rangle$ is not a martingale sequence with zero expectation. Nevertheless, we can control this term from $l(n) \leq L\alpha(n)$ in [Assumption 3.2](#). Specifically, from [Lemma 3.3](#), if $\mathbf{x}(n) \in U$,

$$\|\mathbb{E}_{\mathbf{r}}[F(\mathbf{x}(n), \mathbf{r}, l(n))] - \nabla f(\mathbf{x}(n))\|_2 \leq Ml(n)^2d/2,$$

$$\mathbb{E}_{\mathbf{r}}[\|F(\mathbf{x}(n), \mathbf{r}, l(n))\|_2^2] \leq (2d+4)G^2 + M^2l(n)^4d(d+2)(d+4)(d+6)/18.$$

By replacing equations D.24a and D.25 in [32] with

$$2\alpha(n+1)\mathbb{E} \left[\left(\sum_{i=0}^n \alpha(i)\psi(i) \right) \psi(n+1)\mathbf{1}_{J^n} \right] \leq \sqrt{\epsilon} \sqrt{4\epsilon + 2\sqrt{\epsilon}ML^2\alpha(n+1)^2d},$$

and following the same steps in [32, Lemma D.2], we have

$$(6.3) \quad \epsilon\mathbb{P}(J^n \setminus J^{n+1}) \leq \mathbb{E}(R^n \mathbf{1}_{J^{n-1}}) - \mathbb{E}(R^{n+1} \mathbf{1}_{J^n}) + R^* \alpha(n+1)^2,$$

where $R^0 \mathbf{1}_{J^{-1}} = 0$, $l = \max_n l(n)$,

$$R^* = \sqrt{\epsilon} \sqrt{4\epsilon + 2\sqrt{\epsilon}ML^2d} + \left(\frac{1}{2} + 8\epsilon + 4\sqrt{\epsilon} \right) \left[(2d+4)G^2 + \frac{M^2l^4d_4}{18} + G^2 \right],$$

and $d_4 = d(d+2)(d+4)(d+6)$. By telescoping (6.3), we get

$$\epsilon\mathbb{P} \left(\bigcup_{i=0}^n (J^i \setminus J^{i+1}) \right) = \epsilon \sum_{i=0}^n \mathbb{P}(J^i \setminus J^{i+1}) \leq \sum_{n=0}^{\infty} R^* \alpha(n)^2.$$

Then, for E^∞ defined by (4.7), we have

$$\begin{aligned} \mathbb{P}(E^\infty) &= \inf_n \mathbb{P}(E^{n+1}) \geq \inf_n \mathbb{P}(J^n) = \inf_n \mathbb{P} \left(\bigcap_{i=0}^n (J^i \setminus J^{i+1})^c \right) \\ &= \inf_n \mathbb{P} \left(\Omega \setminus \bigcup_{i=0}^n (J^i \setminus J^{i+1}) \right) \geq 1 - R^* \sum_{n=0}^{\infty} \frac{\alpha(n)^2}{\epsilon}. \end{aligned}$$

Thus, if $\sum_{n=0}^{\infty} \alpha(n)^2$ is small enough such that $1 - R^* \sum_{n=0}^{\infty} \frac{\alpha(n)^2}{\epsilon} > 0$ holds, and the initial distance is not too large (i.e., $\mathbf{x}(0) \in U_0$), then we can conclude that E^∞ occurs with a positive probability. \square

Proof of Theorem 4.10. From Lemma 6.2, the boundedness event occurs with a positive probability. Define the events $E^n = \{\mathbf{x}(i) \in U, i = 1, 2, \dots, n\}$ with U defined in (4.7), corresponding indicator function $\mathbf{1}_{E^n}$, and $G = \max_{\mathbf{x} \in U} \|\nabla f(\mathbf{x})\|_2$. Note that $l(n) \leq L\sqrt{\alpha(n)}$ (Assumption 3.2), by Lemma 6.1, we have that

$$\begin{aligned} &\mathbb{E} (\mathbf{1}_{E^{n+1}} \|\mathbf{x}(n+1) - \mathbf{x}^*\|_2^2 - \mathbf{1}_{E^n} \|\mathbf{x}(n) - \mathbf{x}^*\|_2^2 | \mathcal{F}(n)) \\ &\leq \mathbb{E} (\mathbf{1}_{E^n} \|\mathbf{x}(n+1) - \mathbf{x}^*\|_2^2 - \mathbf{1}_{E^n} \|\mathbf{x}(n) - \mathbf{x}^*\|_2^2 | \mathcal{F}(n)) \\ &\leq -\alpha(n)((1 - \sqrt{\theta})\mu - M\theta - 5M\sqrt{\theta})\mathbf{1}_{E^n} \|\mathbf{x}(n) - \mathbf{x}^*\|_2^2 \\ &\quad + 2\alpha(n) \frac{Ml(n)^2d}{2} \frac{(1 - \sqrt{\theta})\mu - M\theta - 5M\sqrt{\theta}}{M} \\ &\quad + \alpha(n)^2 ((2d+4)G^2 + M^2l(n)^4d(d+2)(d+4)(d+6)/18) \\ &\leq -\alpha(n)((1 - \sqrt{\theta})\mu - M\theta - 5M\sqrt{\theta})\mathbf{1}_{E^n} \|\mathbf{x}(n) - \mathbf{x}^*\|_2^2 + M_4\alpha(n)^2, \end{aligned}$$

where $M_4 > 0$ is a constant dependent on $d, \mu, M, G, \theta, \gamma, m, p, L$. By applying Lemma 3.6, we conclude that $\mathbf{1}_{E^\infty} \|\mathbf{x}(n) - \mathbf{x}^*\|_2^2 \leq \mathbf{1}_{E^n} \|\mathbf{x}(n) - \mathbf{x}^*\|_2^2$ converges almost surely to zero. Consequently, conditioned on E^∞ , the Algorithm 3.2 reaches the $\epsilon_{\mathbf{x}}$ -neighborhood of \mathbf{x}^* in a finite number of iterations almost surely. \square

REFERENCES

- [1] E. M. ACHOUR, F. MALGOUYRES, AND S. GERCHINOVITZ, *The loss landscape of deep linear neural networks: a second-order analysis*, Journal of Machine Learning Research, 25 (2024), pp. 1–76.
- [2] C. AUDET AND W. HARE, *Introduction: tools and challenges in derivative-free and blackbox optimization*, in Derivative-Free and Blackbox Optimization, Springer, 2017, pp. 3–14.
- [3] K. BALASUBRAMANIAN AND S. GHADIMI, *Zeroth-order (non)-convex stochastic optimization via conditional gradient and gradient updates*, Advances in Neural Information Processing Systems, 31 (2018).
- [4] S. BONFANTI AND W. KOB, *Methods to locate saddle points in complex landscapes*, The Journal of chemical physics, 147 (2017).
- [5] X. CHEN, S. LIU, K. XU, X. LI, X. LIN, M. HONG, AND D. COX, *Zo-adamm: Zeroth-order adaptive momentum method for black-box optimization*, Advances in Neural Information Processing Systems, 32 (2019).
- [6] A. R. CONN, K. SCHEINBERG, AND L. N. VICENTE, *Introduction to derivative-free optimization*, SIAM, 2009.
- [7] A. CUTKOSKY AND F. ORABONA, *Momentum-based variance reduction in non-convex SGD*, Advances in Neural Information Processing Systems, 32 (2019).
- [8] S. N. DEMING, L. R. PARKER JR, AND M. BONNER DENTON, *A review of simplex optimization in analytical chemistry*, CRC Critical Reviews in Analytical Chemistry, 7 (1978), pp. 187–202.
- [9] W. E, W. REN, AND E. VANDEN-EIJNDEN, *String method for the study of rare events*, Physical Review B, 66 (2002), p. 052301.
- [10] W. E, W. REN, AND E. VANDEN-EIJNDEN, *Simplified and improved string method for computing the minimum energy paths in barrier-crossing events*, Journal of Chemical Physics, 126 (2007), p. 164103.
- [11] W. E AND E. VANDEN-EIJNDEN, *Transition-path theory and path-finding algorithms for the study of rare events*, Annual Review of Physical Chemistry, 61 (2010), pp. 391–420.
- [12] W. E AND X. ZHOU, *The gentlest ascent dynamics*, Nonlinearity, 24 (2011), p. 1831.
- [13] B. ECKHARDT, *Irregular scattering*, Physica D: Nonlinear Phenomena, 33 (1988), pp. 89–98.
- [14] L. FRANCESCHI, P. FRASCONI, S. SALZO, R. GRAZZI, AND M. PONTIL, *Bilevel programming for hyperparameter optimization and meta-learning*, in International conference on machine learning, PMLR, 2018, pp. 1568–1577.
- [15] G. FREDRICKSON, *The equilibrium theory of inhomogeneous polymers*, no. 134 in International Series of Monographs on Physics, Oxford University Press, 2006.
- [16] X. GAO, B. JIANG, AND S. ZHANG, *On the information-adaptive variants of the admm: an iteration complexity perspective*, Journal of Scientific Computing, 76 (2018), pp. 327–363.
- [17] I. GOODFELLOW, Y. BENGIO, A. COURVILLE, AND Y. BENGIO, *Deep learning*, vol. 1, MIT press Cambridge, 2016.
- [18] E. F. GRAMBERGEN, L. LONGA, AND W. H. DE JEU, *Landau theory of the nematic-isotropic phase transition*, Physics Reports, 135 (1986), pp. 195–257.
- [19] G. A. GRAY, T. G. KOLDA, K. SALE, AND M. M. YOUNG, *Optimizing an empirical scoring function for transmembrane protein structure determination*, INFORMS Journal on Computing, 16 (2004), pp. 406–418.
- [20] G. HENKELMAN AND H. JÓNSSON, *A dimer method for finding saddle points on high dimensional potential surfaces using only first derivatives*, The Journal of chemical physics, 111 (1999), pp. 7010–7022.
- [21] K. G. JAMIESON, R. NOWAK, AND B. RECHT, *Query complexity of derivative-free optimization*, Advances in Neural Information Processing Systems, 25 (2012).
- [22] K. JI, Z. WANG, Y. ZHOU, AND Y. LIANG, *Improved zeroth-order variance reduced algorithms and analysis for nonconvex optimization*, in International conference on machine learning, PMLR, 2019, pp. 3100–3109.
- [23] R. JOHNSON AND T. ZHANG, *Accelerating stochastic gradient descent using predictive variance reduction*, Advances in Neural Information Processing Systems, 26 (2013).
- [24] C. T. KELLEY, *Iterative methods for linear and nonlinear equations*, SIAM, 1995.
- [25] J. LARSON, M. MENICKELLY, AND S. M. WILD, *Derivative-free optimization methods*, Acta Numerica, 28 (2019), pp. 287–404.
- [26] Y. LECON, Y. BENGIO, AND G. HINTON, *Deep learning*, Nature, 521 (2015), pp. 436–444.
- [27] Y. LI, Y. TANG, R. ZHANG, AND N. LI, *Distributed reinforcement learning for decentralized linear quadratic control: A derivative-free policy optimization approach*, IEEE Transactions on Automatic Control, 67 (2021), pp. 6429–6444.
- [28] R. LIFSHITZ AND H. DIAMANT, *Soft quasicrystals—why are they stable?*, Philosophical Magazine, 87 (2007), pp. 3021–3030.

- [29] S. LIU, B. KAILKHURA, P. Y. CHEN, P. TING, S. CHANG, AND L. AMINI, *Zeroth-order stochastic variance reduction for nonconvex optimization*, Advances in Neural Information Processing Systems, 31 (2018).
- [30] W. LIU, Z. XIE, AND Y. YUAN, *A constrained gentlest ascent dynamics and its applications to finding excited states of Bose-Einstein condensates*, Journal of Computational Physics, 473 (2023), p. 111719.
- [31] Y. LUO, L. ZHANG, AND X. ZHENG, *Accelerated high-index saddle dynamics method for searching high-index saddle points*, Journal of Scientific Computing, 102 (2025), p. 31.
- [32] P. MERTIKOPOULOS, N. HALLAK, A. KAVIS, AND V. CEVHER, *On the almost sure convergence of stochastic gradient descent in non-convex problems*, Advances in Neural Information Processing Systems, 33 (2020), pp. 1117–1128.
- [33] M. MEZEI AND D. L. BEVERIDGE, *Free energy simulations*, Annals of the New York Academy of Sciences, 482 (1986), pp. 1–23.
- [34] R. M. MINYAEV, W. QUAPP, G. SUBRAMANIAN, P. V. R. SCHLEYER, AND Y. MO, *Internal conrotation and disrotation in H2BCH2BH2 and diborylmethane 1, 3 H exchange*, Journal of Computational Chemistry, 18 (1997), pp. 1792–1803.
- [35] Y. NESTEROV AND V. SPOKOINY, *Random gradient-free minimization of convex functions*, Foundations of Computational Mathematics, 17 (2017), pp. 527–566.
- [36] J. NOCEDAL AND S. J. WRIGHT, *Numerical optimization*, Springer, 1999.
- [37] J. N. ONUCHIC, Z. LUTHEY-SCHULTEN, AND P. G. WOLYNES, *Theory of protein folding: the energy landscape perspective*, Annual Review of Physical Chemistry, 48 (1997), pp. 545–600.
- [38] W. QUAPP AND J. M. BOFILL, *Locating saddle points of any index on potential energy surfaces by the generalized gentlest ascent dynamics*, Theoretical Chemistry Accounts, 133 (2014), pp. 1–14.
- [39] L. M. RIOS AND N. V. SAHINIDIS, *Derivative-free optimization: a review of algorithms and comparison of software implementations*, Journal of Global Optimization, 56 (2013), pp. 1247–1293.
- [40] O. SHAMIR, *An optimal algorithm for bandit and zero-order convex optimization with two-point feedback*, Journal of Machine Learning Research, 18 (2017), pp. 1–11.
- [41] Y. W. SHANG AND Y. H. QIU, *A note on the extended Rosenbrock function*, Evolutionary Computation, 14 (2006), pp. 119–126.
- [42] B. SHI, L. ZHANG, AND Q. DU, *A stochastic algorithm for searching saddle points with convergence guarantee*, arXiv preprint arXiv:2510.14144, (2025).
- [43] J. SNOEK, H. LAROCHELLE, AND R. P. ADAMS, *Practical bayesian optimization of machine learning algorithms*, Advances in Neural Information Processing Systems, 25 (2012).
- [44] H. SU, H. WANG, L. ZHANG, J. ZHAO, AND X. ZHENG, *Improved high-index saddle dynamics for finding saddle points and solution landscape*, SIAM Journal on Numerical Analysis, 63 (2025), pp. 1757–1775.
- [45] H. TRAN, Q. DU, AND G. ZHANG, *Convergence analysis for a nonlocal gradient descent method via directional gaussian smoothing*, Computational Optimization and Applications, 90 (2025), pp. 481–513.
- [46] P. G. WOLYNES, J. N. ONUCHIC, AND D. THIRUMALAI, *Navigating the folding routes*, Science, 267 (1995), pp. 1619–1620.
- [47] J. YIN, Y. WANG, J. Z. CHEN, P. ZHANG, AND L. ZHANG, *Construction of a pathway map on a complicated energy landscape*, Physical Review Letters, 124 (2020), p. 090601.
- [48] J. YIN, L. ZHANG, AND P. ZHANG, *High-index optimization-based shrinking dimer method for finding high-index saddle points*, SIAM Journal on Scientific Computing, 41 (2019), pp. A3576–A3595.
- [49] Y. YU, T. WANG, AND R. J. SAMWORTH, *A useful variant of the davis-kahan theorem for statisticians*, Biometrika, 102 (2015), pp. 315–323.
- [50] J. ZHANG AND Q. DU, *Shrinking dimer dynamics and its applications to saddle point search*, SIAM Journal on Numerical Analysis, 50 (2012), pp. 1899–1921.
- [51] L. ZHANG, Q. DU, AND Z. ZHENG, *Optimization-based shrinking dimer method for finding transition states*, SIAM Journal on Scientific Computing, 38 (2016), pp. A528–A544.
- [52] L. ZHANG, W. REN, A. SAMANTA, AND Q. DU, *Recent developments in computational modelling of nucleation in phase transformations*, NPJ Computational Materials, 2 (2016), pp. 1–9.
- [53] L. ZHANG, P. ZHANG, AND X. ZHENG, *Error estimates for euler discretization of high-index saddle dynamics*, SIAM Journal on Numerical Analysis, 60 (2022), pp. 2925–2944.
- [54] L. ZHANG, P. ZHANG, AND X. ZHENG, *Discretization and index-robust error analysis for constrained high-index saddle dynamics on the high-dimensional sphere*, Science China Mathematics, 66 (2023), pp. 2347–2360.